SPATIAL PATTERNS OF DNA REPLICATION, PROTEIN SYNTHESIS, AND OXYGEN CONCENTRATION WITHIN BACTERIAL BIOFILMS REVEAL ACTIVE AND INACTVIE REGIONS

by

Suriani Abdul Rani

A thesis submitted in partial fulfillment
of the requirements for the degree

of

Master of Science

in

Chemical Engineering

MONTANA STATE UNIVERSITY
Bozeman, Montana

June 2006

© Copyright

by

Suriani Abdul Rani

2006

All Rights Reserved

APPROVAL

of a thesis submitted by

Suriani Abdul Rani

This thesis has been read by each member of the thesis committee and has been found to be satisfactory regarding content, English usage, format, citations, bibliographic style, and consistency, and is ready for submission to the Division of Graduate Education.

Dr. Philip S. Stewart

Approved for the Department of Chemical and Biological Engineering

Dr. Ron Larsen

Approved for the Division of Graduate Education

Dr. Joseph J. Fedock

STATEMENT OF PERMISSION TO USE

In presenting this thesis in partial fulfillment of the requirements for a master's degree at Montana State University, I agree that the Library shall make it available to borrowers under rules of the Library.

If I have indicated my intension to copyright this thesis by including a copyright notice page, copying is allowable only for scholarly purposes, consistent with "fair use" as prescribed in the U.S. Copyright Law. Requests for permission for extended quotation from or reproduction of this thesis in whole or in parts may be granted only by the copyright holder.

Suriani Abdul Rani

August 2006

ACKNOWLEDGEMENTS

This work was supported by W. M. Keck Foundation.

I would like to thank numerous people who have helped me throughout my undergraduate and graduate studies here at MSU: Dr. Phil Stewart for his support and guidance; Betsey Pitts for her training and wonderful cookies; colleagues in the Control Lab; and my family for their wonderful support, and not asking me for payments, yet.

Not to forget Shelly Thomas, Administrative Assistant at the Chemical and Biological Engineering Department for taking care of her 'high-maintenance' child; Raaja Raajan Angathevar Veluchamy and Haluk Beyenal for helping out with the microelectrode; Kelli Buckingham-Meyer and John Neumann for taking time on assisting me with the respirometer.

TABLE OF CONTENTS

TABLE OF CONTENTS - CONTINUED

LIST OF FIGURES

LIST OF TABLES

ABSTRACT

Biofilms harbor both active and inactive cells and it is a challenge to characterize the spatial and population heterogeneity of specific activities within a biofilm. Spatial patterns of DNA replication and protein synthetic activity were imaged by techniques developed using staphylococcal systems. The first technique measures DNA synthetic activity by pulse-labeling with the thymidine analog 5-bromo-2-deoxyuridine (BrdU) followed by immunofluorescent detection of brominated DNA. The second technique makes use of an inducible green fluorescent protein construct that can be used to detect the capacity for de novo protein synthesis. These techniques were applied to biofilms grown in three different reactor systems. In all cases, measurements revealed that even in simple single-species biofilms, complex spatial distributions of anabolic activity occur. In a colony biofilm system, two distinct regions of DNA synthetic activity were observed, one close to the nutrient interface and another adjacent to the air interface. A similar pattern was measured by GFP induction. The dimensions of DNA synthetic activity ranged from 25 to 31 μm and the average protein synthetic activity ranged from 36 to 38 μm at the air interface. When pure oxygen was introduced, a wider zone of active DNA replication (45 μm) and GFP synthesis (59 μm) was measured at the gas interface. Oxygen penetration calculated (26μm) corresponds with the zones of respiratory activity (19 to 38 μm), DNA synthetic activity and protein synthetic activity measured at the air interface. The dimensions of DNA synthetic activity and protein synthesis activity at the nutrient interface ranged from 13 μm to 19 μm. The addition of glucose to the media increased the zone of protein synthesis at the nutrient interface to 33 μm. Stratified patterns of activity were also observed in biofilms developed in two continuous flow reactors. While biofilms harbor regions of active anabolism, the techniques also demonstrate that these biofilms contain regions of complete inactivity. Such inactive zones may contribute to the special ecology of biofilms and tolerance to antimicrobial agents. The techniques, particularly BrdU labeling, are generic and may find application to many microbial biofilm systems.

INTRODUCTION

Biofilms

Biofilms are dense aggregates of microorganisms that attach and colonize biotic and abiotic surfaces and can be composed of single or multi-species microbes. The biofilm life cycle includes attachment, colonization, growth, and detachment. Bacteria initiate biofilm growth in response to specific environmental cues, such as nutrient availability (Rice et al., 2005). Bacterial cells undergo a transition from free-floating cells to surface attached cells in response to a nutrient-rich medium. The biofilms continue to colonize the surface until they are nutrient deprived, upon which they detach from the surface in search of a nutrient source (O'Toole et al., 2000).

Bacterial biofilms are often associated with the excretion of extracellular polymeric substance (EPS) (Donlan, 2002**;** Toledo-Arana et al., 2005) , which has slimy, glue-like properties that protects bacterial cells from host defense mechanisms and antimicrobials, thus facilitating resistance towards antimicrobials.

The demonstrated resistance of bacterial biofilms to antimicrobials has caused problems in human health and in numerous industries causing medical and economic consequences. Biofilms are found everywhere and have significant impacts on medical implants (Costerton et al., 1999; Stewart and Costerton, 2001), drinking water (Martiny et al., 2005), food processing (Timke et al., 2005), and even oil recovery systems (Zhu et al., 2003; Bryant et al., 1991). However, its planktonic counterpart does not demonstrate

similar resistance towards antimicrobial agents. The complete mechanism for biofilm resistance still remains unclear.

There are several phenomena that are postulated to contribute to biofilm resistance. One explanation is that antimicrobials do not penetrate biofilms completely. However, from a study recently done (Rani et al., 2005), antimicrobials the size of antibiotics and biocides do penetrate biofilms by diffusion rapidly, unless neutralizing reactions are present.

Another postulate for biofilm tolerance is the presence of an altered microenvironment region deep within a biofilm which is different from the bulk fluid. This region may harbor cells that are growing slowly or not at all in the interior of the biofilm (Xu et al., 2000). Since most antibiotics target macromolecule synthesis processes, it is plausible that non-growing cells could be less susceptible to killing. Metabolically inactive bacteria could also be less vulnerable to other types of chemical and physical challenges. As envisioned in Figure 1.1, a biofilm might contain rapidly-growing cells, but also cells that are growing slowly, cells that have entered a stationary-phase-like state, and cells that are completely dormant. A biofilm could contain some bacteria growing aerobically and others growing fermentatively. If this conjecture is correct, even a single biofilm cell cluster could comprise a population spanning a spectrum of physiological states. These different states may be due to local variation in the availability of nutrients and electron acceptors, or to mechanisms such as phenotypic variation.

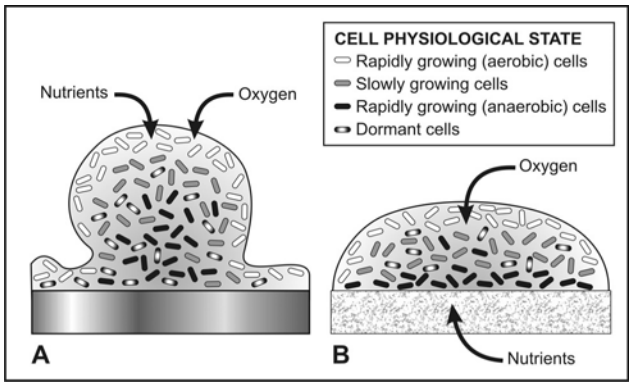

Figure 1.1. Hypothesized heterogeneity of physiological status in microbial biofilms. Panel A illustrates a scenario in which microorganisms have colonized an impermeant, non-nutritive surface (e.g., a catheter, a water pipe). Panel B illustrates a scenario in in scenario in which microorganisms receive nutrients through the attachment surface (e.g., a burn wound, a lettuce leaf). Illustrated by P. Dirckx.

There is some evidence for substrate limitation and slow growth in staphylococcal biofilms. The average specific growth rate of bacteria in a biofilm can be calculated by dividing the overall rate of production of bacteria by the standing population of cells in the biofilm. Using this approach, Hodgson et al. (1995) found that *Staphylococcus aureus* grew with a specific growth rate of 0.06 h^{-1} in biofilms whereas it grew with a specific growth rate of 0.7 h^{-1} in the planktonic state in the same medium. The community-averaged growth rate of *Staphylococcus epidermidis* in colony biofilms was 0.035 h^{-1}, much lower than the maximum specific growth rate of 0.82 h^{-1} measured in batch culture (Zheng and Stewart, 2002). These results suggest that the average growth rate in a staphylococcal biofilm may be only a few percent of the growth rate exhibited in conventional suspended-culture conditions. DNA microarray comparisons of transcriptional patterns in biofilms and planktonic cells reveal a general down-regulation

of transcription, translation, and aerobic energy production (Yao et al., 2005) and up-regulation of anaerobic metabolism (Beenken et al., 2004).

A limitation of all of the preceding studies with staphylococci is that they reveal none of the heterogeneity in growth state and activity that is probably present in the biofilm population. These studies provide only whole-population averages. Consider that a biofilm in which the average specific growth rate is half the growth rate of planktonic cells might actually consist of a population of cells in which half are growing rapidly and half not at all. The average does not accurately represent either of the subpopulations. However, spatial patterns of growth activity in bacterial biofilms in other microorganisms such as *Escherichia coli*, *Pseudomonas aeruginosa*, and *Klebsiella pneumoniae* have been investigated extensively. Approaches included the induction of alkaline phosphatase in response to phosphate starvation (Huang et al, 1998; Xu et al., 1998; Xu et al, 2000), oligonucleotide probing of ribosomal RNA content (Poulsen et al., 1993), green fluorescent (GFP) expression (Sternberg et al.,1999; Werner et al., 2004), radioisotope labeling and autoradiography (Stewart et al., 1991; Stewart and Robertson, 1988), fluorescently labeled monoclonal antibody (Stewart et al., 1997), and nucleic acid staining based on RNA-DNA content (Wentland et al., 1996). These studies have demonstrated gradients in biological activities in biofilms.

Gram-Positive Bacteria and Biofilm Infections

Gram positive cocci, such as *Staphylococcus epidermidis* and *Staphylococcus aureus* are common human pathogens that cause a variety of serious infections (*S. epidermidis* is an inhabitant of the skin and is considered to be an opportunistic pathogen, whereas *S. aureus* colonizes mainly the nasal passages and should always be considered a potential pathogen. Gram-positive infections are hard to treat with current antibiotic treatments due to the high-level natural resistance to antimicrobials (O'Toole et al., 2000). Staphylococci also form thick, highly heterogeneous biofilms within a few days. For these reasons, *S. epidermidis* and *S. aureus* were selected for this research.

Staphylococcus epidermidis and *Staphylococcus aureus*

S. epidermidis and *S. aureus* are responsible for biofilm related nocosomial infections (O'Toole et al., 2000; O'Gara and Humphreys, 2001). They are the most prevalent organisms responsible for persistent infections following various medical surgeries including surgical vascular grafts (Costerton et al., 1999), orthopedic devices (Costerton et al., 1999; Nishimura et al., 2006), and prosthetic-joints (Stewart and Costerton, 2001; Zimmerli et al., 2006). Biofilm infections develop gradually, and may be slow to produce overt symptoms. Once established, most staphylococcal infections result in acute disease due to the varied range of virulence factors that contribute to their pathogenesis. Excretion of exotoxins and tissue degrading enzymes are among the significant virulence factors. Bacterial persistence and recurring infections are also

generally observed, especially in patients with indwelling medical devices. Biofilm infections commonly persist until the infected device is surgically removed from the body.

The emergence of staphylococcal strains with antibiotic resistance and the capability of colonizing implanted medical devices have further complicated the treatment of device-related infections. This has lead to an increase in research in the development and implementation of therapeutic approaches and efficient infection control measures (O'Gara and Humphreys, 2001).

Biofilm Ecology

Mature biofilms often have a complex architecture within which gradients in the concentrations of metabolic substrate and producsts create niches that affect the constituents and the community structure of a biofilm. Consequently biofilms often provide a living environment appropriate to diverse types of microorganisms. In regions where oxygen is available and can diffuse into the biofilm, aerobic populations thrive. At depths where oxygen is limited or absent, anaerobes predominate. Some microbial populations consume the metabolic waste products of others, and so they are found in close proximity with the waste producers. Nutrient limitation in the interior of a biofilm can induce the bacterial cell to transition from exponential growth to a slow or no-growth state, which is usually accompanied by an increase in resistance towards antimicrobials. t is well known that starving bacterial cells can be much less susceptible to a variety of antimicrobial agents (Mah and O'Toole, 2001).

Confocal Scanning Laser Microscopy

Confocal scanning laser microscopy (CSLM) is powerful imaging tool for studying biofilms. Images are generated by scanning the laser beam across the specimen (Herman, 2001). The advantage of utilizing CSLM is that out-of-focus blur is in essence absent from confocal images, direct non-invasive observation of fully hydrated biofilms can be performed and the generation of three-dimensional (3D) images is possible through the collection of serial optical sections from thick specimens (Sheppard and Shotton, 1997; Wilson, 2002).

In conventional microscopes, the out-of-focus blur is contributed from the illumination of the entire object field simultaneously, which excites fluorescence emissions throughout the whole depth of the sample, rather than just the focal plane (Wilson, 2002). Much of the light collected by the objective lens to form the image will come from regions of the sample above and below the selected focal plane, thus reducing contrast and clarity of the image. This differs greatly from CSLM, as CSLM utilizes single point illumination at the focal plane which requires scanning in order to build up an image of the entire specimen. The insertion of a pin-hole aperture in the optical system results in almost all the light originating from regions above and below the focal plane of a CSLM being physically rejected from contributing to the observed image, thus increasing contrast and sharpness of the image (Sheppard and Shotton, 1997).

The CSLM approach is innocuous and non-invasive. Unlike electron microscopes that require more elaborate cell-processing procedures and in general are limited to thin or

sectioned specimens, direct observation of fully hydrated biofilms can be performed using CSLM thus retaining the physical properties of the biofilm.

In a thick specimen, parts of the specimen outside the focal plane are blurred in conventional microscopes. In CSLM, only the part of the specimen within the focal region is imaged which produces a sharp image. Clearly, the specimen can be sectioned optically without having to resort to mechanical means. In this way, confocal microscopes have the ability to obtain an in-focus series of images, which may then be used to reconstruct the original volume of specimen at high resolution, thus allowing the generation and analysis of three-dimensional architecture of the specimen (Wilson, 2002).

The maximum usable thickness of samples in conventional light microscopes is limited to well-flattened cultured cells, which ranges from 2 to 10 μm, before the fluorescence in the specimen away from the region of interest interferes with resolution of structures in focus (Sheppard and Shotton, 1997; Paddock, 1999). Furthermore, CSLM provides a slight increase in both lateral and axial resolution with a theoretical maximum resolution of 0.2 μm (Herman, 2001).

The use of the CSLM has extended to a great number of applications in many areas of current research interest due to high-quality images obtained from easily prepared samples for conventional light microscopes. Furthermore, the accessibility of laser light sources, low cost and more user friendly computer image and data processing systems have increased the popularity of CSLM (Inoué, 1995).

In this research, a confocal epi-fluorescence microscope was used. This microscope differs slightly from a single-channel confocal microscope, in that it is equipped with three lasers capable of delivering an appropriate range of excitation wavelengths. By the use of fluorescence microscopy, one can attach a fluorescence dye molecule to a specimen are a marker to visualize the fluoresced structure using a specific excitation light. Different molecules display distinct excitation and emission spectra, which can be selectively used for the analysis of molecular structures by utilizing filters to select wavelengths of excitation and emission (Herman, 2001). This allows visualizing more than one dye at the same time.

Time-lapse confocal imaging was also utilized in this research via collection of single optical sections at specified time intervals.

5-Bromo-Deoxyuridine (BrdU) Labeling

About 30 years ago, Albert Castro, M.D., produced a polyclonal antibody that was specific for BrdU and Howard Gratzner, Ph.D. developed the first monoclonal antibody to BrdU. It is important to note that this useful work was also accomplished by other fellow investigators. By specific determination of S-phase content and timing in the cell cycle, one could devise better killing of tumor cells with chemotherapeutic drugs. The development of detection and quantification of DNA synthesis using BrdU labeling has facilitated cell cycle studies thus providing a better technique to help treat cancer (Leif et al., 2004; Dolbeare et al., 1983).

Today, this assay is being use for various applications. 5-bromodeoxyuridine (BrdU) labeling has been used extensively in the study of both eukaryotic (Elias et al., 2002; Oike et al., 2006; Lichtenwalner et al., 2006) and bacterial cells (Pernthaler et al., 2002; Artusson et al., 2005; Pernthaler and Pernthaler, 2005).

Incorporation of the thymidine analog, BrdU, into DNA during DNA synthesis in place of the native nucleotide provides a marker for proliferating cells (Kuhn et al., 1991). Labeled DNA is subsequently illuminated with a fluorescently labeled monoclonal antibody that specifically recognizes brominated DNA. The rate of incorporation of BrdU into genomic DNA is unknown and may be different from species to species. It was reported that thymidine (TdR) was replaced by BrdU at a rate of 25% in *Bacillus subtilis* DNA (Pernthaler et al., 2002).

In this research, BrdU labeling of staphylococcal biofilms was developed using the colony biofilm system (Anderl et al., 2000; Zheng and Stewart, 2002; Walters et al., 2003). The protocol in this investigation was modified from elsewhere (Dolbeare et al., 1994).

Green Fluorescent Protein Expression

The green fluorescent protein (GFP) was derived from jellyfish *Aequorea victoria*, although other bioluminescent organisms can be found as well. The fluorescence is produced by sequential activation of aequorin and GFP. Upon binding to calcium, aequorin emits blue light which consecutively excites GFP to emit green fluorescence. Because GFP is such a powerful tool, it has been used in numerous applications including

GFP as a reporter for gene expression, as a marker to study cell lineage during development, and as a tag to localize proteins in living cells (Gerdes and Kaether, 1996). In this research, GFP is used as a marker for protein synthetic activity. This method utilizes a tetracycline-induced promoter to induce GFP expression (Bateman et al, 2001). Chloramphenicol was added to the *S. aureus* inoculum to ensure retention of the plasmid.

Tetracycline and Chloramphenicol

Tetracycline and chloramphenicol are 'broad spectrum' antibiotics effective against a wide range of gram-positive and gram-negative bacteria. Both tetracycline and chloramphenicol are categorized in the group of bacteriostatic, in which it reversibly inhibits the growth of bacteria. Tetracycline blocks bacterial protein synthesis (translation) by reversibly binding to the 30S ribosome and inhibit binding of aminoacyl-t-RNA to the acceptor site on the 70S ribosome (Chopra and Roberts, 2001). Chloramphenicol binds to the 50S ribosome and inhibits peptidyl transferase activity. Some of the bacterial infections that can be treated by using tetracycline are pneumonia, severe acne, and urinary tract infections. Tetracycline is also a common alternative drug for patients who are allergic to penicillin. Chloramphenicol however is effective against typhoid fever and meningitis.

Plasmids with Inducible Promoters

The reporter gene gfp_{uvr} was cloned downstream of the *xyl/tetO* (tetracycline inducible) promoter. Restriction enzymes were used to cleave the *tetR* (encoding tetR repressor) and *xyl/tetO* promoter from pWH353 was inserted into *S. aureus-E. coli* shuttle

vector (pKS236). Correct insertion into the recombinant plasmid was confirmed by restriction mapping and sequencing. The plasmid pALC2073 was produced from pSK236 containing the *tetR* gene and the *xyl/tetO* promoter that were cleaved from pWH353 and cloned into the *Pst*I and *Sma*I sites. The gene, gfp_{uvr}, was cloned into the *Eco*RI site downstream from the inducible promoter in pALC2073 to produce pALC2084. The strain ALC2085 contains RN6390 containing pALC2084 (pALC2073::*gfpuvr*) (Zhang et al., 2000; Bateman et al., 2001).

Thesis Goal

The goal of this thesis is to investigate integrated application of techniques to map spatial patterns of DNA synthesis, protein synthesis, and local oxygen concentration that enable the visualization and quantification of highly heterogeneous patterns of respiratory and anabolic activity in *S. epidermidis* and *S. aureus* biofilms.

MATERIALS AND METHODS

Bacteria and Media

S. epidermidis strain RP62A (ATCC 35984) and *S. aureus* strain RN6390 containing pALC2073::*gfpuvr* (ALC2085) were grown on tryptic soy broth (TSB) at 37°C. The GFP gene contained in this *S. aureus* strain was under the control of a tetracycline-inducible promoter (Bateman et al. 7851-57). Full strength TSB (30 g of broth powder per liter of deionized water) was used to grow shake flask cultures that provided the inoculum for biofilm experiments.

Biofilm Reactors

Colony Biofilm Preparation

Colony biofilms were grown on polycarbonate membranes resting on agar plates (Werner et al. 6188-96) as shown in Figure 2.1. Planktonic cultures of *S. epidermidis* and *S. aureus* were grown overnight in TSB and diluted to an optical density of 0.050 (at 600 nm, with a 1-cm path length). Chloramphenicol (10 μg/ml) was added to the medium used to grow the *S. aureus* inoculum to ensure retention of the plasmid. Chloramphenicol was not included in the agar medium used to grow colony biofilms. One 10-μl drop of diluted planktonic culture was used to inoculate membranes (25-mm, 0.22 μm pore size; Osmonics INC, Minnetonka, MN) resting on tryptic soy agar (TSA) plates at a concentration of 40 g of broth powder per liter of deionized water. The membranes were sterilized by UV exposure (10 min per side) prior to inoculation. The

plates were inverted and incubated at 37°C, and the membranes were transferred to a fresh TSA plate every 24 h and were grown for 44 h. For the *S. epidermidis* strain, the biofilms were transferred to agar medium containing 1mM BrdU for an additional 4 h. For the *S. aureus* strain, the biofilms were transferred to agar medium containing 1 μg/ml tetracycline for an additional 4 h.

Colony biofilms were subjected to various nutrient and oxygen conditions during the introduction of BrdU or tetracycline. For anaerobic growth experiments, agar plates were transferred into an anaerobic incubation pouch with a sealing bar (BBLTM GasPakTM Pouch, Becton, Dickinson and Company, Sparks, MD) in an anaerobic glove box (Coy Laboratory Products Inc., Ann Arbor, MI). In some experiments, TSA was supplemented with glucose at 2.5 g/L. To supply additional oxygen, agar plates were placed in a bag that was inflated with pure oxygen and sealed.

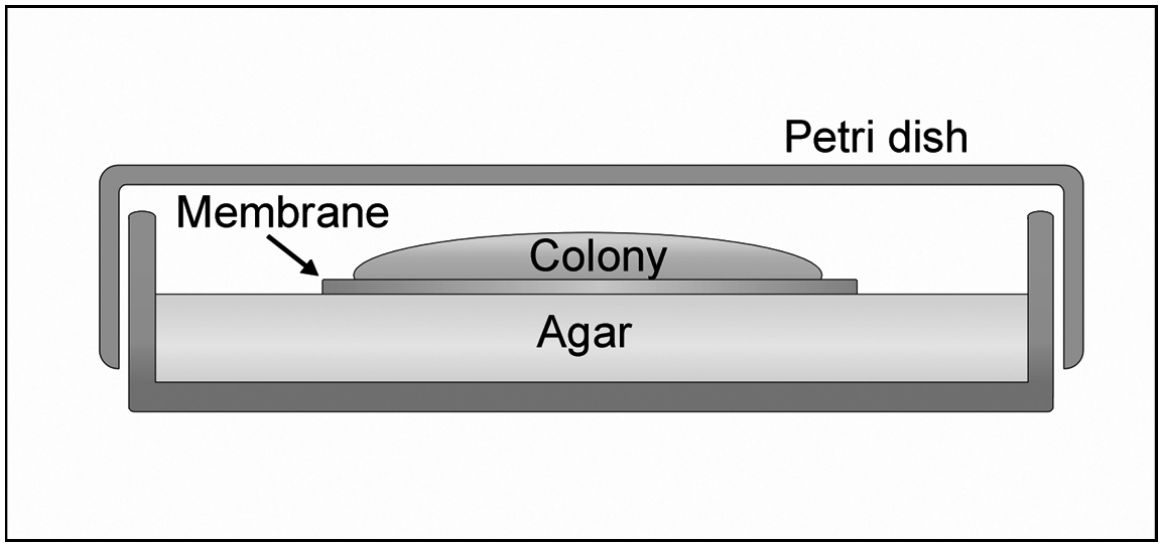

Figure 2.1. Colony biofilm growth setup.

Planktonic Culture Preparation

Planktonic batch cultures of *S. epidermidis* were grown overnight at 37°C in baffled flasks in TSB. BrdU (1mM) was added to fresh medium inoculated with 50-fold dilution of overnight culture after 1.5 h of growth for exponential phase experiments and after 7 h of growth for stationary phase experiments. For a killed control experiment, an overnight culture was autoclaved for 20 minutes prior to the introduction of BrdU. Planktonic cultures were grown for a total of 11 h prior to filtration onto a polycarbonate membrane using a filtration unit.

Capillary Biofilm System

Biofilms were grown in glass capillary tubes (Friedrich and Dimmock, Millville, New Jersey) under continuous flow conditions (Werner et al. 6188-96); Rani et al., 2005) as shown in Figure 2.2. The glass tubes had square cross sections which allowed direct

microscopic observation of the biofilm through the tube walls. The capillary tubes had a nominal inside dimension of 0.9 mm and were approximately 10 cm long. Capillaries were inoculated with 2 ml of overnight cultures of *S. epidermidis* or *S. aureus*, and flow was stopped for 4 h. Chloramphenicol (10 μg/ml) was added to the medium used to grow the *S. aureus* inoculum. No antibiotic was included in the medium used to grow the *S. aureus* capillary biofilm. After 4 h static incubation, the flow of medium (1/10th strength TSB) was initiated at a flow rate between 120 and 180 mL/h by gravity feed. This flow rate corresponds to a Reynolds number of 37 to 56 based on the hydraulic radius of the clean tube. The medium carboy and the capillary were placed in separate 37°C incubators stacked on top of each other. Biofilms were allowed to develop for 20 h prior to the introduction of medium containing 1mM BrdU for an additional 4 h or 1 μg/ml tetracycline for an additional 7 h. For microscopic observation, capillary biofilm was placed in a holder (Biosurface Technologies, Bozeman, MT) that could be mounted onto the microscope stage.

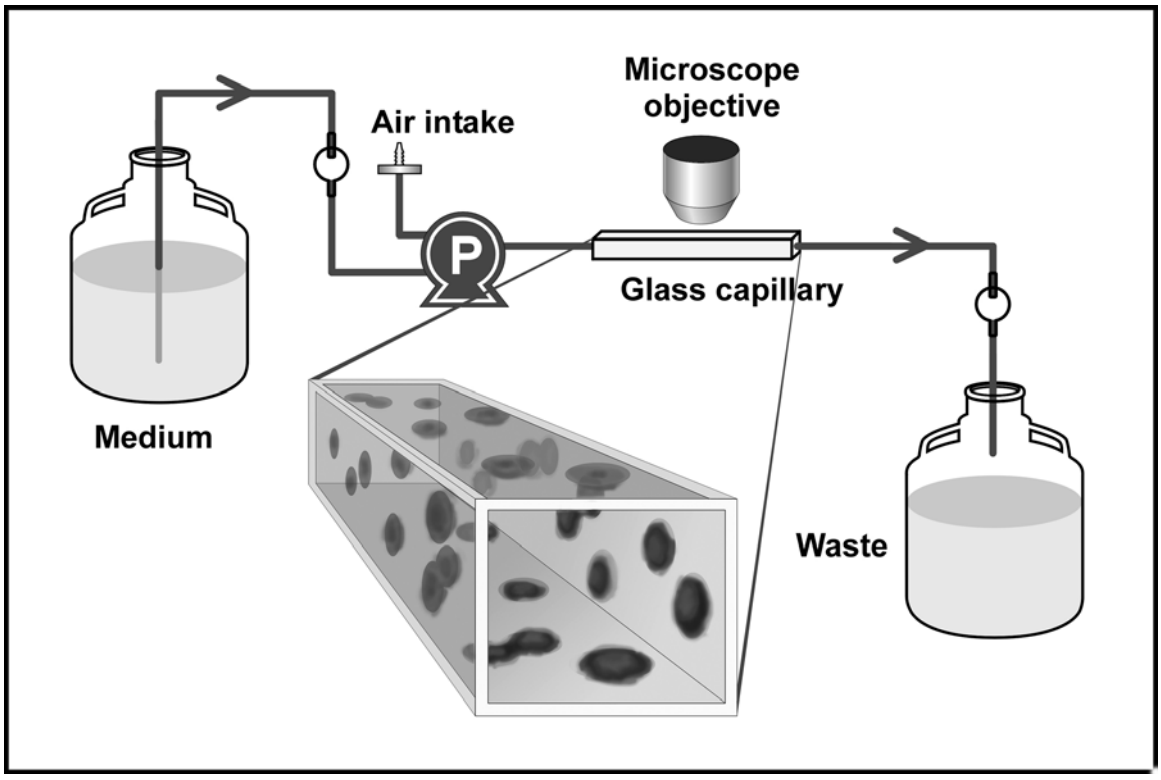

Figure 2.2. Capillary biofilm growth setup.

Drip-flow Biofilm System

Drip-flow biofilm reactors were used to cultivate biofilms (Xu et al. 4035-39)) as shown in Figure 2.3. Stainless steel coupons (7.8 cm x 1.2 cm) were inclined at a 10° angle within the reactor which was incubated at 37°C. After inoculation with an overnight culture of *S. epidermidis* or *S. aureus*, the reactor was allowed to stand for 24 h. Chloramphenicol (10 μg/ml) was added to the medium used to grow the S. aureus inoculum. No antibiotic was included in the medium used to grow the S. aureus drip flow biofilm. After this time, the flow was initiated and the medium (1/10th strength TSB) dripped onto the coupons from a height of approximately 1 cm. For the *S. epidermidis* strain, the reactor was fed for 20 h at a flow rate of 10 ml/h before switching

to medium containing 1mM BrdU for an additional 4 h. For the *S. aureus* strain, the reactor was fed for 44 h at a flow rate of 10 ml/h before switching to medium containing 1 μg/ml tetracycline for an additional 4 h.

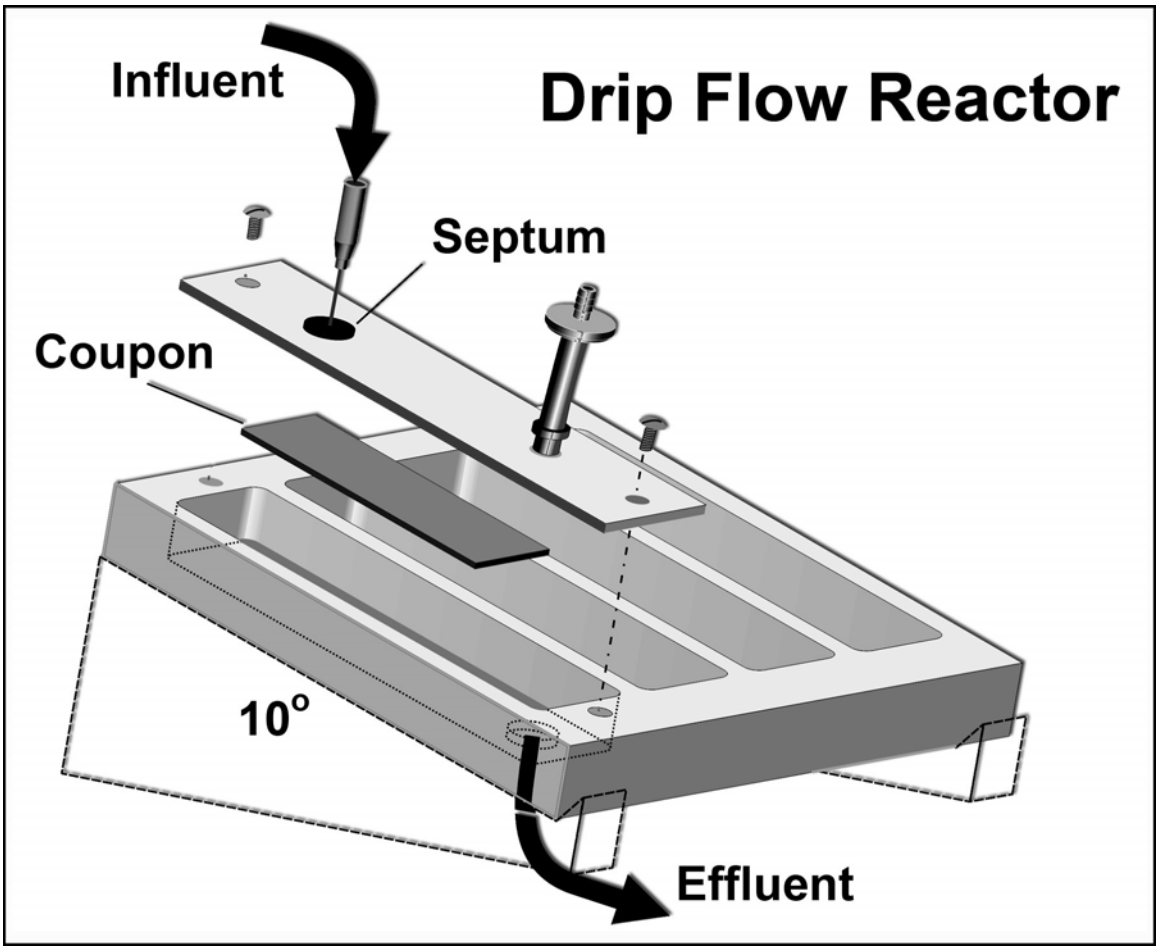

Figure 2.3. Drip flow biofilm growth setup.

Cryoembedding and Cryosectioning

Colony biofilm, drip-flow biofilm, and planktonic culture samples were cryoembedded with Tissue-Tek O.C.T. compound (VWR Scientific Products, West Chester, PA) as described previously (Wentland et al. 316-21); Werner et al., 2004). Membrane-supported biofilms were placed on a 7.8 cm x 1.2 cm stainless steel coupon and the colonies were covered with the embedding medium. The coupon was placed on dry ice and the medium was allowed to freeze. Colonies along with the membranes were removed from the coupon and the edges of the membranes were trimmed. The colonies with the embedded side down were placed on the dry ice and the embedding medium was used to cover the exposed membranes, which was then allowed to freeze. Embedded colonies were sectioned into 5-μm thick cross sections using a Leica CM 1850 cryostat. The colony cross sections were placed on Superfrost Plus microscope slides (Fisher Scientific).

DNA Synthetic Activity

The BrdU technique described in this paper was a modification of a published protocol (Methods in Cell Biology 297-316). *S. epidermidis* colony cross sections were fixed for 5 min using a solution containing 80% ethanol in water. This fixation process was to stop metabolic activity and fix the sections onto the slides.

A solution of 50 mg/L lysozyme was introduced for 5 min to permeabilize the cell envelope. Subsequently, 4N hydrochloric acid was introduced for 10 min to denature

DNA as this protocol only recognizes single stranded DNA. A blocking solution of 2% skim milk and 0.3% Tween 80 in Tris-buffered saline (TBS) was introduced for 5 min to limit non-specific binding of antibody.

A 20-fold dilution factor of anti-bromodeoxyuridine, mouse IgG1, monoclonal PRB-1, Alexa Fluor® 488 conjugate (anti-BrdU, Alexa Fluor® 488 conjugate) was introduced which illuminated regions of active replication in green fluorescence. Slides were covered to protect from photo-bleaching the antibody. Sections were probed with the antibody for one hour. Sections were counterstained with 5 mg/L rhodamine B for 5 min (Eastman Organic Chemicals, Rochester, New York) to reveal the extent of the biomass independent of its activity in red fluorescence. Sections were stained by placing 20 μl drops in succession along the cross section. After each step, slides were rinsed twice with phosphate buffer solution (PBS) with excess solution blotted from the slide. Slides were fixed and stained at room temperature.

After introduction of BrdU for 4 h, glass capillary biofilms were processed with the same series of reagents detailed above and directly observed with confocal scanning laser microscopy (CSLM). Experiments were also conducted in which a capillary biofilm was labeled with BrdU for 4 h, cryoembedded, cryosectioned, and stained prior to observation with CSLM.

Drip flow biofilms were grown for 24 h prior to labeling with BrdU for 4 h, cryoembedded, cryosectioned, stained, and then examined by CSLM.

Protein Synthetic Activity

S. aureus colony biofilms were grown for 44 h, transferred to a TSA plate containing 1 μg/ml tetracycline for 4 h, cryoembedded, and cryosectioned into 5 μm slices using a Leica CM 1850 cryostat.

After 20 h of growth, *S. aureus* capillary biofilms were exposed to 1 μg/ml tetracycline for 4 h, and were directly observed with time lapse CSLM to obtain a time series of GFP expression during induction with tetracyline.

Drip flow biofilms were grown for 44 h prior to the introduction of 1 μg/ml tetracycline for 4 h, cryoembedded, cryosectioned, and then examined by CSLM.

Some experiments were performed where both BrdU and tetracycline were introduced simultaneously to image DNA and protein synthesis in the same *S. aureus* colony. Colony biofilms were grown for 44 h which were then transferred to a TSA plate containing 10 mM BrdU and 1 μg/ml tetracycline. Images of frozen sections were first obtained in the green channel for GFP expression. The slides were then heat-treated followed by the fixation and staining protocol to image DNA synthetic activity. These steps abolished fluorescence due to GFP. A second set of images was taken to image DNA replication, which was also obtained in the green channel. Images were re-aligned and combined to view the combined activities. Since protein synthesis and DNA replication were both initially imaged in the green channel, DNA replication images were false-colored in red.

Several *S. aureus* controls were performed by inducing colony biofilms after 44 h of growth with tetracycline for an additional 4 h. The membrane was removed from the agar plate and was placed in a test tube containing 9 ml phosphate buffer solution. The test tube was vortexed for 5 min to remove cells from the polycarbonate membrane. A 10-µl drop of dispersed cells was placed on a microscope slide and scanned for GFP expression as described below. A second control was performed. Colony biofilms were allowed to develop for 44 h then removed from the agar plate and was placed in a test tube containing 9 ml phosphate buffer solution. The test tube was vortexed for 5 min to remove cells from the polycarbonate membrane then induced with tetracycline for 4 h. A 10-µl drop of dispersed cells was placed on a microscope slide and both slides were directly observed using fluorescence microscopy. Images were obtained in two channels (transmission and green channel) and were color combined in order to visualize single cells with and without green fluorescence, whereby cells exhibiting protein synthesis are expressed in green fluorescence. Image thresholding methods were not used in this experiment. Cells with and without GFP expression on both slides were counted and compared.

Oxygen Penetration

Oxygen concentration profiles in colony biofilms were measured with a dissolved oxygen microelectrode as described elsewhere (Werner et al., 2004) and diagrammed in Figure 2.4. The dissolved oxygen microelectrode was based on the principle of the common amperometric ‘Clark-type’ oxygen sensor. The electrode is composed of four

main parts; an outer casing, a working electrode (cathode), a counter electrode (anode) which is also known as the reference electrode, and an oxygen-permeable silicone membrane. Oxygen diffuses through the membrane to the region between the membrane and the cathode. This reaction consumes electrons, produces a current in the circuit, and consumes oxygen surrounding the close proximity of the electrode. The current from the cathode is proportional to the surface area of the electrode and the rate with which the oxygen molecules arrive at the cathode, which is in turn proportional to the concentration of oxygen in the bulk external solution.

In this research, Ag/AgCl half-cell was used as the reference electrode and a noble metal, platinum was used as the working electrode. The apparatus was housed in an incubator at 37°C. The casing was fabricated from a Pasteur pipette that was tapered down to an active sensor tip between 10 and 20 μm. A buffered electrolyte solution consisting of 0.3 M K_2CO_3, 0.2 M $KHCO_3$, and 1 M KCl filled the internal cavity. Two electrodes occupied the internal cavity as well; a gold-plated tip, glass-encased platinum cathode at which oxygen diffusing in through the silicone membrane was reduced and a silver-silver chloride counter electrode, which served as the current return. A potential of approximately –0.8 volts of direct current was applied between the working electrode and the counter electrode. The electrode was calibrated in air, and a zero level was obtained by placing the electrode tip in a beaker of distilled water bubbled with nitrogen gas for half an hour. Calibration was performed at 37°C. The data was fitted using the calibration curve to generate oxygen concentration profiles. The local reaction rate of oxygen was calculated from measured oxygen concentration profiles by evaluating the second

derivative with a central difference formula. The width of the respiratory zone was taken as the distance from the biofilm-air interface to the distal edge of the oxygen reaction rate peak as measured at the peak half-height.

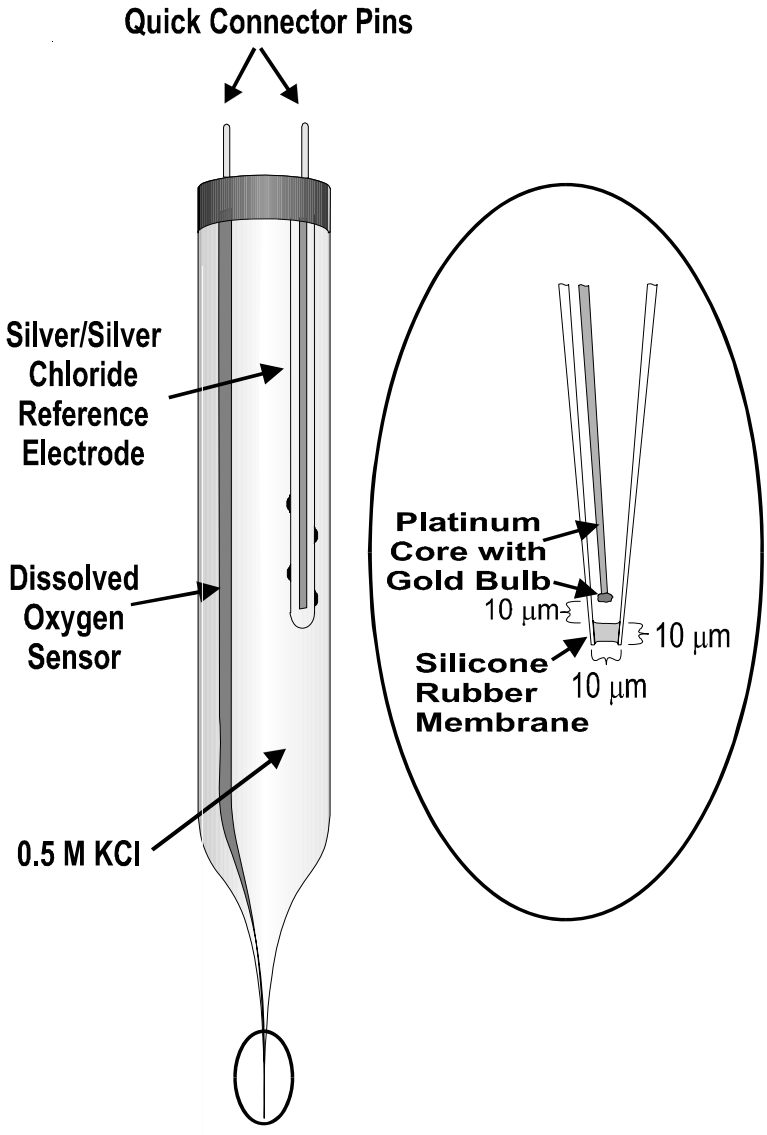

Figure 2.4. Dissolved oxygen microelectrode.

Respirometry

Respirometry involves the measurement of changes in the concentration of gases (e.g. oxygen, carbon dioxide, hydrogen sulfide and methane) in a sample within an enclosed head space. The system can be used in aerobic systems for oxygen uptake measurement and in anaerobic systems to measure methane and/ or carbon dioxide production. The periodic measurements of gas concentration and volume of the head space allow calculations of incremental and accumulated values of the consumption and production of gases. Respirometer systems are highly efficient and sensitive with the capability of detecting the activity of less than 100 cells in a sample. A maximum of 20 samples can be measured simultaneously. Some of the major drawbacks in running a respirometer system are: it cannot differentiate one microorganism from another; it will measure the respiration of a population as a whole, samples must be hermetically enclosed to prevent external inflow or outflow of gas into the reactor; and samples producing water vapor effects calculations by increasing total gas volume and diluting the concentrations of gases in the system. Respirometers can be used to measure respiratory activity of microorganism in batch cultures (flask or agar plate). The caps of flasks and lids of agar plates were designed so as to that gas passage is possible only through the tubes connected to the respirometer.

The rate of oxygen consumption in colony biofilms was measured using a Micro-OxymaxTM ‘Closed Circuit’ Respirometer (Columbus Instrument, Columbus, Ohio). Seven colony biofilms in nutrient agar bottles were attached to the respirometry

equipment. A set of control was performed in which the nutrient agar bottle did not contain a colony biofilm. The rate of oxygen consumption data was obtained at an interval of 1.5 h for a total of 48 h. Between 15 h and 20 h, colony biofilms grown independently were measured, frozen, and sectioned to determine the area and thickness of colony biofilm. The colony area was computed by measuring the average diameter of the colonies with the assumption that colony biofilms are circular. The thickness of colonies was determined by sectioning and measuring the average thickness of the cross sections microscopically. The rate of oxygen consumption between 15 h and 20 h was averaged and was divided by the average volume of colony biofilms. This value corresponds to the volumetric reaction rate which was used to predict oxygen penetration depth. The software MicroOxymax was used to collect data.

Plasmid Stability

S. aureus biofilm was tested for the stability of the GFP-bearing plasmid. A biofilm covered membrane was aseptically removed from the agar plate and was placed in a test tube containing 9 ml phosphate buffer solution. The test tube was vortexed for 5 min to remove cells from the polycarbonate membrane. The resulting suspension was serially diluted in PBS before spread plating. Dispersed cells were spread plated on a TSA plate and TSA plate supplemented with 10 μg/ml chloramphenicol. Agar plates were inverted and incubated at 37°C. Colony-forming units (CFU) in both plates were determined and the experiment was repeated twice. A sterile toothpick was used to take a

single dab from one CFU from the TSA spread plate and dabbed on both TSA plate and TSA plate containing 10 μg/ml chloramphenicol. Agar plates were inverted and incubated at 37°C. Up to 100 CFUs (using a sterile toothpick each time) were used to conduct the colony screening experiment. CFUs in both plates were compared.

Microscopy and Image Analysis

Confocal scanning laser microscopy was performed with a Leica TCS NT confocal scanning laser microscope (Werner et al. 6188-96). For imaging in transmission mode, excitation from a 488-nm laser was used. For imaging DNA synthesis and GFP expression, a 488-nm laser was used and the emission was collected at 500 to 530 nm (green channel). For imaging rhodamine B, a 568-laser was used and the emission was collected at 585 to 615 nm (red channel). A 10X dry objective lens was used for these experiments. Microscope images were analyzed using the linescan function in MetaMorph image analysis software (Universal Imaging Corporation, Downingtown, PA). For colony and drip flow biofilm experiments, the relative fluorescent intensities were measured for at least three independently grown biofilms and for three independent sections across each biofilm. Intensity profiles were measured perpendicular to the membrane supporting the colony biofilm. The dimension of active zones of DNA synthesis or protein synthesis was taken as the width of peak at the peak half-height. Statistical tests were performed using a two-sided t-test. The biofilm thickness was measured as the distance from the membrane to the biofilm-air interface. For the *S.*

aureus capillary biofilm experiment, a time series was initiated in which an image was collected every 2 min. The time series ran for 4 to 7 h.

Statistical Analysis

Statistical comparisons were made using a two-sided t-test assuming unequal variances. In order to utilize the two-sample t- test, the data from two random samples should be normally distributed (symmetric, bell-shaped distribution) and from independent observations (values in one sample does not influence the other sample). Hypothesis tests include two hypotheses: the null hypothesis (H0) and the alternative hypothesis (H1). The null hypothesis is the initial claim and is often specified using previous research or general knowledge and is tested against the alternative hypothesis. The alternative hypothesis is what one assumes to be true or expects to prove true. The t-test provides two statistics that one can use to perform a test of the difference between means: a t-value and a p-value. The t-value is used to obtain the p-value and the p-value is the measure of discrepancy between the hypothesized value for a population and the observed sample. For a two-tailed test, p-values are the sum of areas in the two tails.

The commonly used value of α-level (level of significance) of 0.05 was selected for this research, which implies a 95% confidence level. This also means that the chance of finding an effect that does not really exist is only 5%. If the p-value is less than or equal to α-level, the null hypothesis (H0) is rejected with 95% confidence and it is concluded that the population means are not the same, and claim support for the alternative hypothesis (H1), which indicates the means are statistically significantly

different (unequal). If the p-value is greater than α-level, one fails to reject H0 and can not claim that the population means are not the same (can not claim support for H1) (Devore and Peck, 2005). In this research, Minitab 14 statistical software was used.

RESULTS

Mapping Patterns of DNA Synthesis in Biofilms

S. epidermidis formed well established colony biofilms after 48 h of incubation and extensive, heterogeneous biofilms in drip flow reactor and glass capillary tubes after 20 h of incubation. These biofilms proved to be appropriate models for the analysis of DNA synthesis.

BrdU labeling of staphylococcal biofilms using the colony biofilm system was developed. The colony biofilm system is made up of dense aggregates of bacteria that develop on a filter membrane resting on a nutrient agar plate. Carbon and nitrogen sources, and other required substrates, are delivered to the bottom of the biofilm from the agar. Oxygen is delivered to the top of the biofilm via air. The geometry of this system resembles that illustrated in Figure 1.1. After 44 h of development, mature colony biofilms were transferred to a BrdU labeled plate for 4 h, then frozen, sectioned, and probed with anti-BrdU antibody. Highly stratified patterns of DNA synthetic activity, representative images of which are shown in Figure 3.1, were observed. After 48 hr of development, the mean thickness (and standard deviation) of *S. epidermidis* colony biofilms was 153 ± 18 μm. The colony biofilms that were not labeled with BrdU but were probed with antibody did not appear to have green fluorescence (Figure 3.1A). Colony biofilms labeled with BrdU but not probed with the antibody likewise exhibited no fluorescence (image not shown). Since *S. epidermidis* is a facultative microorganism, it is able to metabolize by both respiration and fermentation. When grown in air, two distinct

bands of DNA synthetic activity were observed close to the nutrient and air interfaces, respectively (Figure 3.1B). Occasionally there was also a trace of activity in a centrally located stratum. Slow-growing or non-growing cells were observed in the interior of the biofilms.

These experiments also demonstrate that BrdU was able to diffuse out of the agar, through the membrane, and permeate throughout the colony biofilm during the 4 h labeling period. The evidence is clear by the incorporation of BrdU into cells at the opposite side of the biofilm from which this substrate was delivered.

Several *S. epidermidis* planktonic controls were labeled with BrdU for 4 h in suspension then filtered the cells onto a membrane. The membranes were treated like colony biofilms where they were processed for antibody probing. One batch of planktonic controls was labeled with BrdU at exponential phase and was expected to have higher DNA synthetic activity than a culture that was labeled with BrdU for 4 h at stationary phase. This was demonstrated with the bright green fluorescent intensity in exponential phase and relatively weak green fluorescent intensity in stationary phase (images not shown). When BrdU was added after the planktonic culture was killed by heat treatment, no DNA synthesis should occur. This was shown with no green fluorescence exhibited (image not shown). These planktonic experiments were another set of controls to reinforce the interpretation that green fluorescence indicates active DNA synthesis.

Spatial Patterns of DNA Synthesis are Highly Stratified in Biofilms

Highly stratified patterns of DNA synthetic activity were observed in all three biofilm reactors where BrdU labeling was utilized. The dimensions of the zones of DNA synthetic activity were quantified by image analysis (Table 3.1). When colony biofilms were grown in air, the zone of DNA synthesis at the air interface averaged 31 μm and the zone of DNA synthesis at the nutrient interface averaged 13 μm. The difference in the dimensions of these two zones was statistically significant ($P < 0.001$).

Patterns of DNA synthetic activity in *S. epidermidis* colony biofilms by BrdU labeling changed in response to changes in the nutrient and oxygen conditions. When the biofilm was subjected to anaerobic conditions during the BrdU labeling, the DNA synthetic band at the air interface was eliminated and DNA synthesis was only observed at the nutrient interface (Figure 3.1C). When pure oxygen was introduced during the BrdU labeling, a thicker DNA synthetic band was observed at the air interface (Figure 3.1D). The expansion in the DNA synthetic band at the air interface increased from 31 μm in air to 46 μm in pure oxygen, a factor of 1.5, was statistically significant ($P < 0.001$). Overall, the dimension of the zone of DNA synthetic band along the nutrient interface did not change significantly as the gaseous environment was changed from anaerobic, to air, to pure oxygen ($P = 0.37$ and $P = 0.10$ for aerobic to anaerobic and aerobic to pure oxygen comparisons, respectively). When glucose was added to the agar during the BrdU labeling, variability in patterns was observed, but generally enlarged regions of DNA synthetic activity were observed, probably due to the presence of non-

growing or dead cells (image not shown). These specimens did not lend themselves to image analysis because the activity patterns were so irregular.

Biofilms grown under continuous flow conditions in glass capillary tubes were labeled with BrdU, probed with anti-BrdU antibody, were examined in situ by confocal scanning laser microscopy. Green fluorescent rings, corresponding to DNA synthetic activity, were observed at the surfaces of cell clusters (Figure 3.2A). In places where the biofilm was very thin, all of the biomass was bright green suggesting intense DNA synthetic activity. In larger cell clusters, no DNA synthetic activity could be detected in the interior of the cluster.

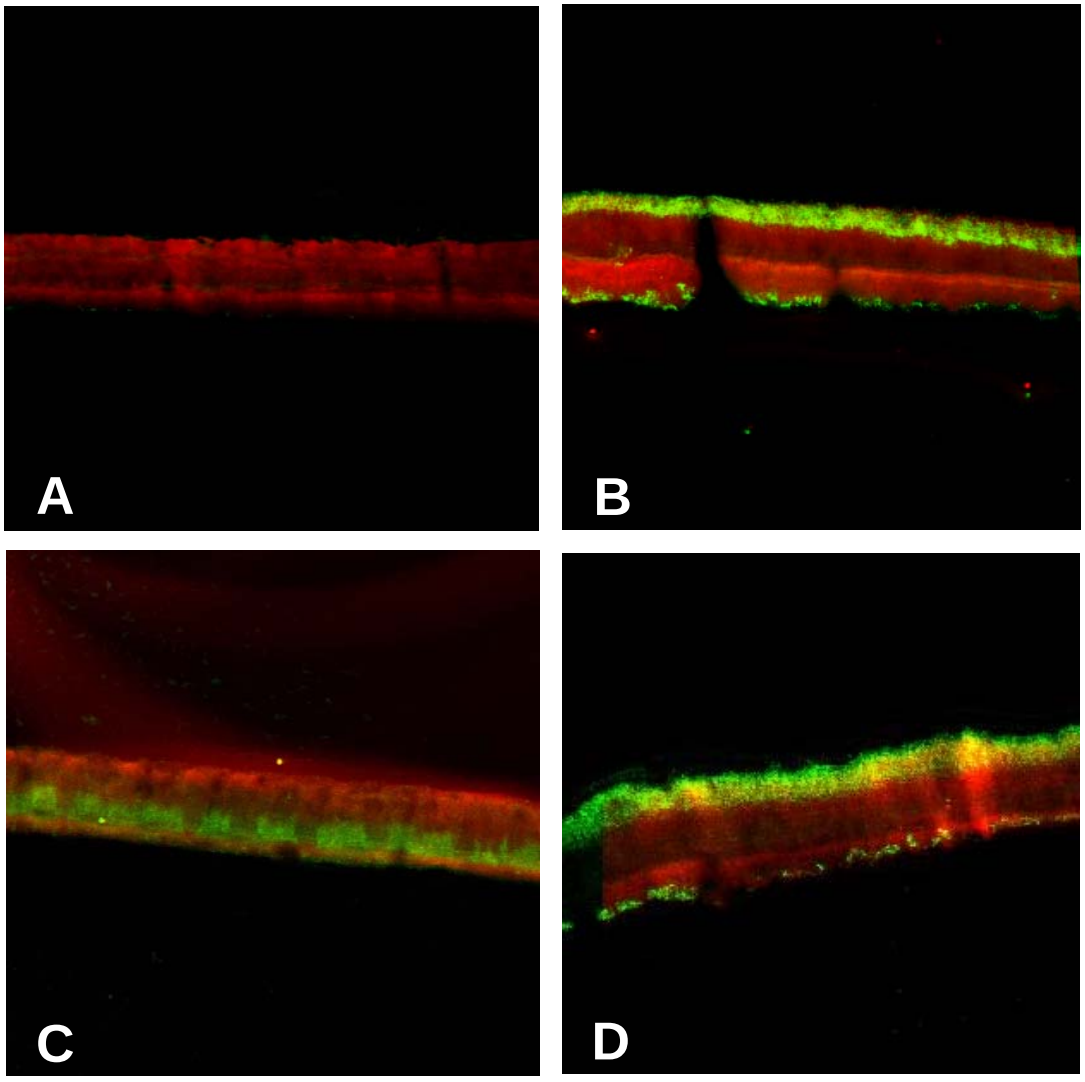

Figure 3.1. Patterns of DNA synthesis in *S. epidermidis* colony biofilms. Panel A shows an unlabeled (no BrdU) colony biofilm probed with antibody. Panel B shows a colony biofilm labeled with BrdU under aerobic conditions. Panel C shows a colony biofilm labeled with BrdU under anaerobic conditions. Panel D shows a colony biofilm labeled with BrdU in an environment of pure oxygen. Green areas are due to BrdU incorporation into DNA and indicate active replication. Red areas are due to rhodamine B counterstaining that reveals the extent of the biomass independent of its activity. In each image, the membrane interface of the colony is on the bottom and the air interface on the top.

The probability of whether these patterns could be an artifact of incomplete permeation of the antibody into the biofilm was questioned. The first set of controls was performed by extending the antibody incubation period from 4 h to10 h in glass capillary biofilms (image not shown). Similar patterns of DNA synthesis were observed when compared to patterns of DNA synthesis in biofilms probed with antibody for 1 h. A second set of controls was performed. A BrdU-labelled capillary biofilm was perfused with a tissue embedding medium and frozen on dry ice. The glass was chipped away with a triangular file, and the specimen was sectioned. Frozen sections were probed with anti-BrdU antibody (image not shown). Though this procedure disturbs biofilm structure, it yielded stratified patterns qualitatively consistent with those shown in Figure 3.2A. This suggests that the zone of DNA activity observed in capillary biofilms was not limited by penetration of antibody into cell clusters.

Biofilms grown in another continuous flow system, the drip flow reactor, and labeled with BrdU at the end of the growth period also exhibited a stratified pattern of DNA synthetic activity. A single band of bright green fluorescence was observed at the air interface which averaged 39 μm in width. No activity was observed at the substratum (Figure 3.2B).

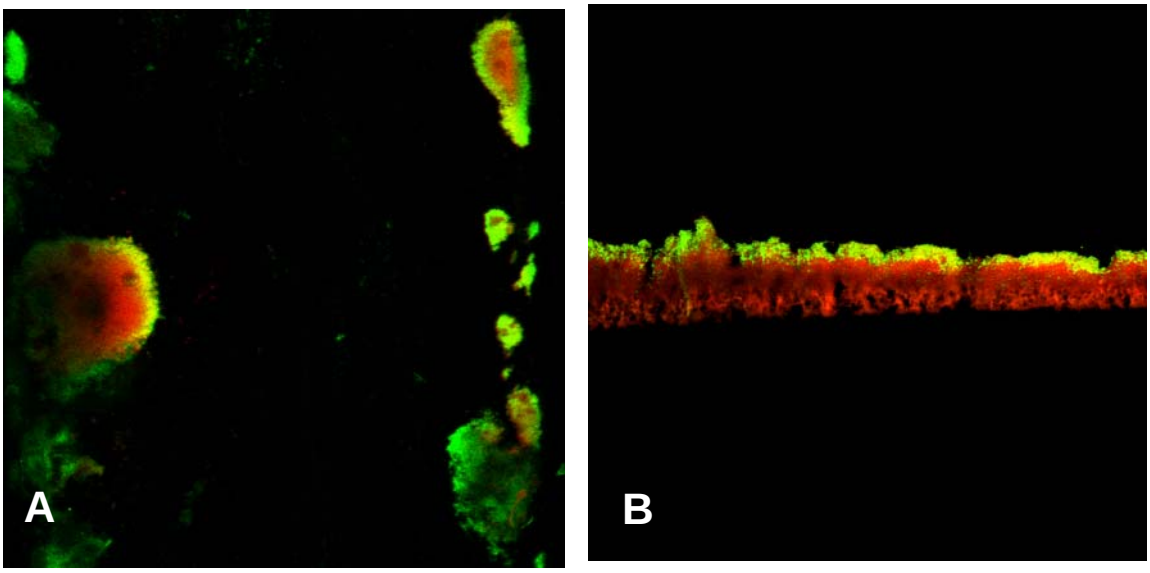

Figure 3.2. Patterns of DNA synthesis in *S. epidermidis* capillary (A) and drip flow (B) biofilms. Green areas are due to BrdU labeling and red areas are due to rhodamine B counterstain. Flow was from top to bottom in panel A. In panel B, the substratum was on the bottom and the air interface on the top.

Mapping Patterns of Protein Synthesis in Biofilms

S. aureus formed well established colony biofilms and hearty drip flow biofilms after 48 h of incubation, and extensive, heterogeneous biofilms in glass capillary tubes after 20 h of incubation. These biofilms proved to be appropriate models for the analysis of protein synthesis.

The cellular capacity for de novo protein synthesis using a *S. aureus* strain containing a tetracycline-inducible green fluorescent protein (GFP) was visualized (Bateman et al., 2001). In the presence of sub-inhibitory concentrations of tetracycline, bacterial cells that can synthesize protein make GFP and thus can be imaged by fluorescence microscopy. *S. aureus* colony biofilms induced with tetracycline for 4 h

appeared to have bands of green fluorescence indicating patterns of protein synthetic activity when cross sections were examined (Figure 3.3). The mean thickness (and standard deviation) of 48-h-old *S. aureus* colony biofilms was 173 ± 22 μm.

This inducible GFP construct is plasmid borne, so it is important to establish the stability of the plasmid. Dark regions of a biofilm could be regions in which there is no protein synthesis occurring, or they could just be regions in which most of the bacteria have lost the plasmid. To address this issue, colony biofilms were dispersed and the cell suspension was plated onto TSA and also onto TSA containing 10 μg/ml chloramphenicol. The number of colonies that formed on the antibiotic-containing plates was 94% of the number that grew on TSA plates. One hundred colonies from the TSA plates were picked and spotted onto chloramphenicol-containing plates. All 100 colonies grew in the presence of chloramphenicol, indicating that these bacteria contained the plasmid. These results show that the plasmid is retained in most or all of the cells in biofilms.

The inducing agent, tetracycline, was delivered to the colony biofilm from the membrane interface and was able to induce expression of protein synthesis at the opposite edge of the biofilm from which this agent was delivered, indicating that tetracycline was able to permeate throughout the colony biofilm during the 4 h induction period (Figure 3.3A).

The populations of dead (X_D), active viable (X_A), and inactive viable (X_I) cells in a staphylococcal biofilm were analyzed. Several *S. aureus* colony biofilms were induced with tetracycline and then the bacterial cells were dispersed. Other colony biofilms were

dispersed and then induced with tetracycline. Cells that were dispersed before inducing with tetracycline had a higher percentage of 57% of total cells with GFP expression ($X_A + X_I$). Cells that were induced with tetracycline and then dispersed had a lower percentage of 34% of total cells with GFP expression. This indicates that in an intact biofilm 34% of total cells are viable and active (X_A), 23% of the total cell population is viable but not producing GFP expression (X_I) in intact biofilms and 43% of the biofilm is dominated by dead cells (X_D). X_{TOT} represents total cells. This analysis is summarized by the equations below.

$$X_{TOT} = X_D + X_A + X_I$$

$$\frac{X_A + X_I}{X_{TOT}} = 0.57$$

$$\frac{X_A}{X_{TOT}} = 0.34$$

$$\frac{X_I}{X_{TOT}} = 0.23$$

$$\frac{X_D}{X_{TOT}} = 0.43$$

Spatial Patterns of Protein Synthesis are Highly Stratified in Biofilms

Highly stratified patterns of protein synthetic activity were observed in all three biofilm reactors when the inducible GFP technique was utilized. The dimensions of the zones of protein synthetic activity were quantified by image analysis (Table 3.1). When colony biofilms were grown in air, the zone of protein synthesis at the air interface averaged 38 μm and the zone of DNA synthesis at the nutrient interface averaged 14 μm (Figure 3.3A). The difference in the dimensions of these two zones was statistically significant ($P < 0.001$).

Patterns of protein synthetic activity in *S. aureus* colony biofilms measured by GFP induction changed in response to changes in the nutrient and oxygen conditions (Table 3.1). When the biofilm was subjected to anaerobic conditions during the tetracycline induction, the protein synthetic band at the air interface was eliminated and protein synthesis was only observed at the nutrient interface (Figure 3.3B). When pure oxygen was introduced during the BrdU labeling, a thicker DNA synthetic band was observed at the air interface (Figure 3.3C). The expansion in the DNA synthetic band at the air interface from 38 μm in air to 59 μm in pure oxygen, a factor of 1.6, was statistically significant ($P < 0.001$). When the agar was supplemented with glucose during the tetracycline induction period, a thicker band of protein synthetic activity was observed at the nutrient interface which averaged 33 μm, whereas there was no significant change in the dimension of the zone of GFP expression at air interface (Figure 3.3D). The expansion in the zone of protein synthetic activity at the membrane interface

from 14 μm in medium deficient in glucose to 33 μm in medium supplemented with glucose was statistically significant ($P < 0.001$).

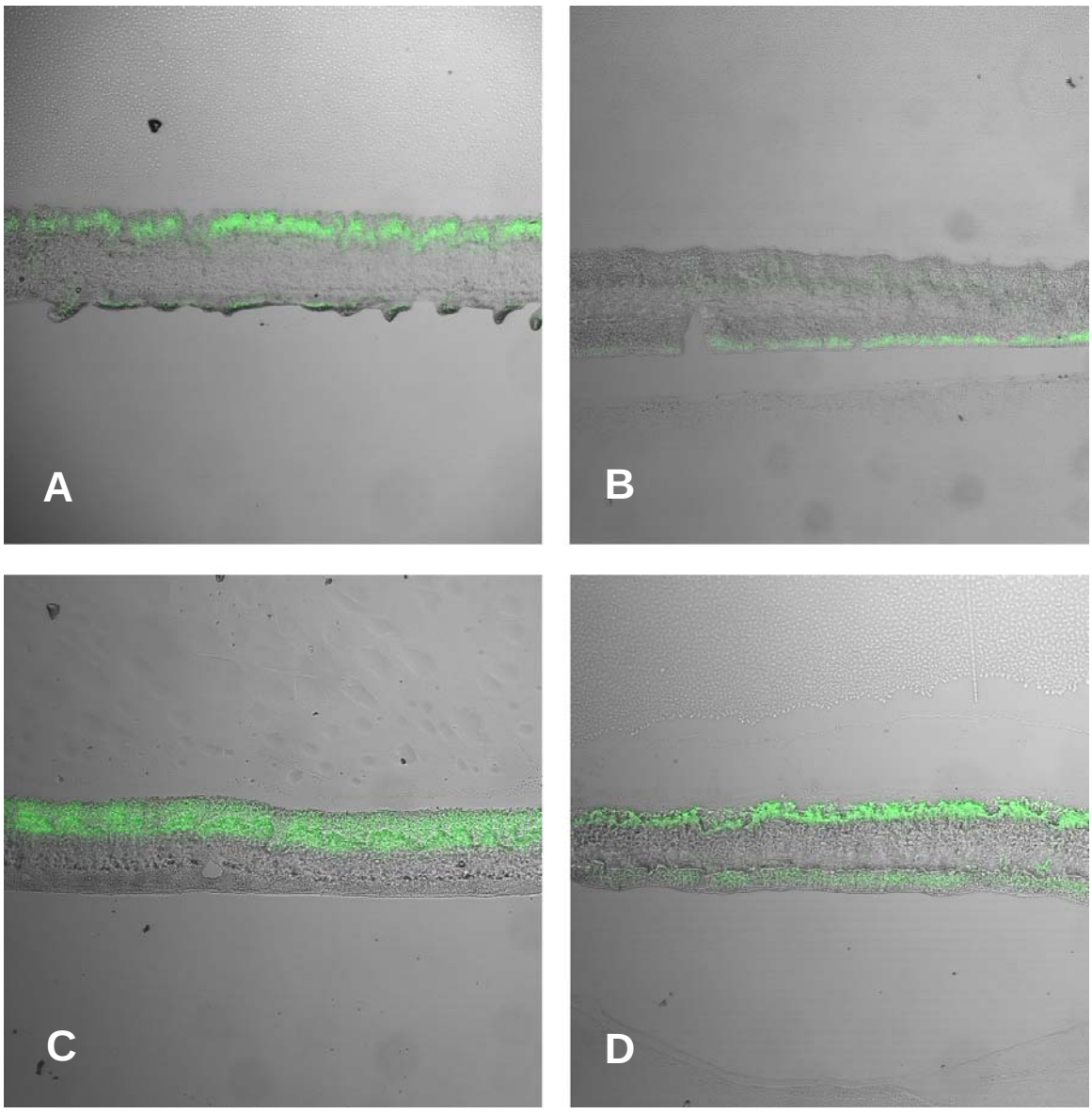

Figure 3.3. Patterns of protein synthetic activity (green) imaged in *S. aureus* colony biofilms induced for GFP expression in air (A), on mediums supplemented with glucose (B), in pure oxygen (C), or in anaerobic environment (D). Transmission overlay shows the extent of the biomass independent of activity.

Experiments were also conducted where *S. aureus* colony biofilms were simultaneously labeled with BrdU and induced for GFP expression by adding tetracycline. A sequential imaging approach was used because the protocol for preparing specimens for antibody probing destroys GFP fluorescence. Frozen sections were imaged for GFP fluorescence immediately after sectioning and prior to processing for immunofluorescence. A transmitted light image of the section was also collected. The slide was removed from the microscope and processed for antibody probing. This processing includes treatment with hydrochloric acid which eliminates all GFP fluorescence. After probing with antibody, the fluorescence pattern corresponding to DNA synthetic activity was imaged. This image was false colored red to distinguish it from the GFP signal (Figure 3.4A). The two fluorescent images were overlaid with an image analysis software using structural features visible in transmitted light images to align them. Stratified patterns of DNA synthetic activity and protein synthetic activity were observed and these patterns coincided closely with each other (Figure 3.4B).

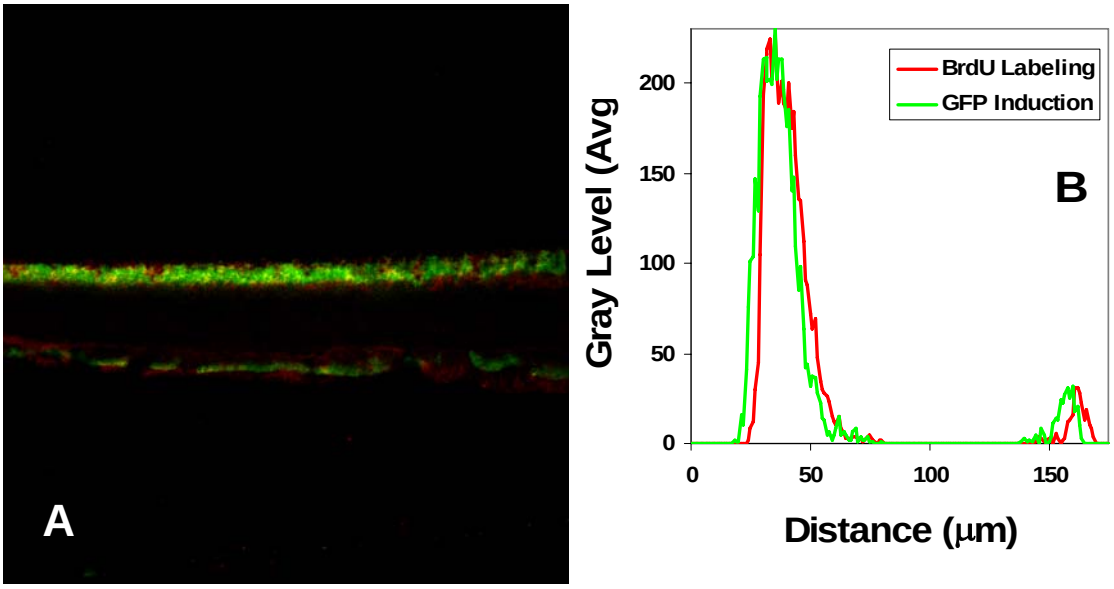

Figure 3.4. Patterns of DNA synthesis and GFP expression in the same *S. aureus* colony biofilm. In Panel A, the substratum is on the bottom, with the air interface on the top. Panel B shows the average fluorescent intensity along a linear transect across the section. Green areas are due to GFP expression and red areas are due to BrdU labeling.

The transient expression of GFP in *S. aureus* biofilms grown in capillary reactors was imaged (Figure 3.5). After growing the biofilm for 24 h, tetracycline was added to the medium. Fluorescence first appeared at the periphery of the cell clusters adjoining the fluid flow. GFP fluorescence progressively moved inward toward the center of the cluster, but did not ever develop in the center of a large cell cluster in the course of the 7 h tetracycline induction period (Figure 3.5). Image analysis of the green fluorescent intensity at several different locations in the biofilm demonstrates the large variation from spot to spot in the local rate of protein synthesis (Figure 3.6).

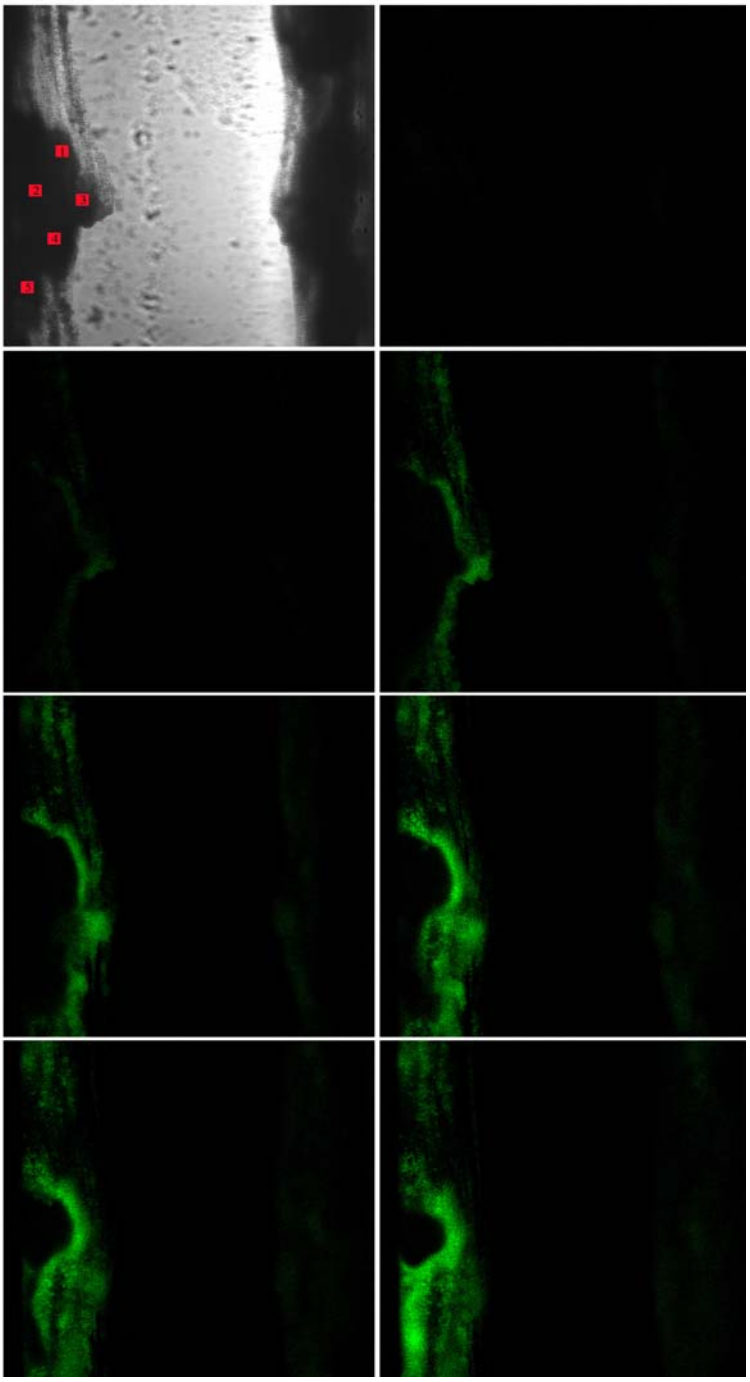

Figure 3.5. Time series of GFP expression in *S. aureus* biofilm during tetracycline induction in a capillary reactor biofilm. The time is indicated in hours, after the first appearance of tetracycline in the flow cell. Panel A shows a transmission image of the cell cluster. Green areas are due to GFP expression. Flow was from top to bottom.

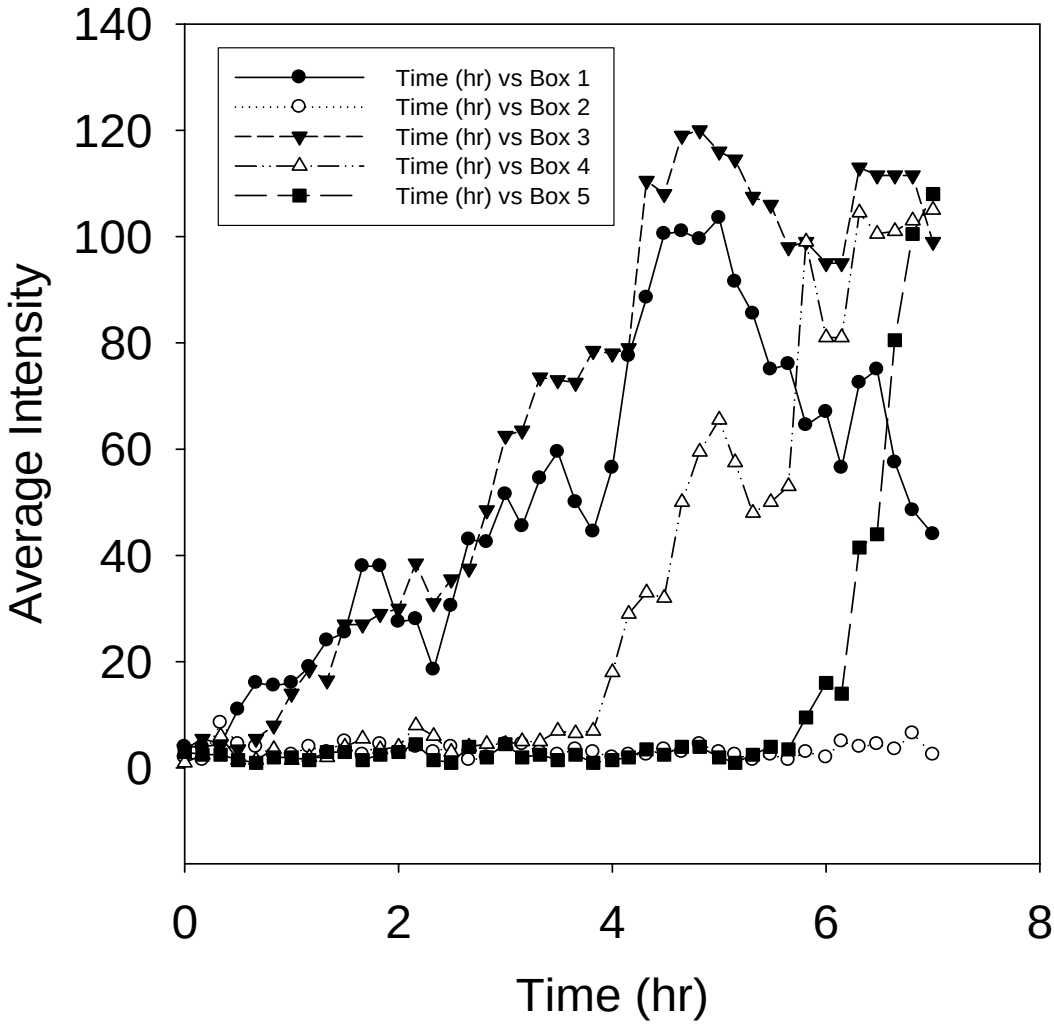

Figure 3.6. Variable dynamics of GFP expression during induction in *S. aureus* biofilm. Each numbered curve corresponds to a different spot in the biofilm as indicated by the boxes in Figure 6A. The pixel intensity in the area indicated by the box was averaged at each time point.

Biofilms grown in another continuous flow system, the drip flow reactor, induced with tetracycline also exhibited a stratified pattern of protein synthetic activity. A single band of bright green fluorescence was observed at the air interface which averaged 41 μm and none at the substratum (Figure 3.7).

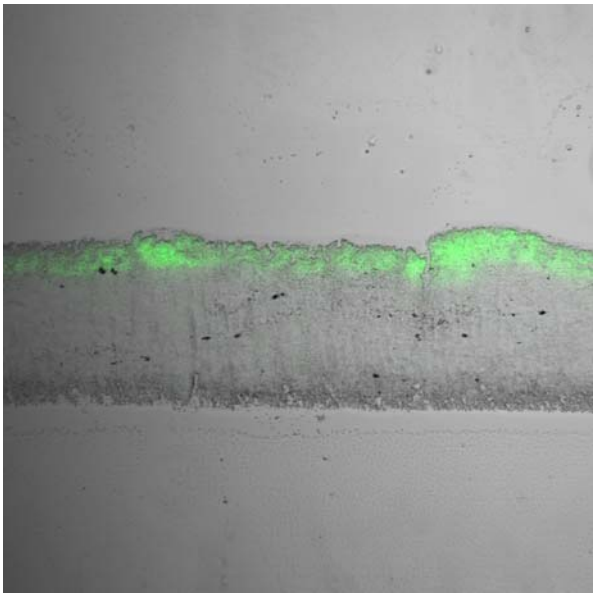

Figure 3.7. Patterns of protein synthesis in *S. aureus* drip flow biofilm. The substratum was on the bottom and the air interface on the top.

Condition	*S. epidermidis* DNA replication		*S. aureus* protein synthesis		*S. aureus* DNA replication	
	Gas (μm)	Membrane (μm)	Gas (μm)	Membrane (μm)	Gas (μm)	Membrane (μm)
Air	31 ± 14	16 ± 11	38 ± 9	14 ± 5	25 ± 8	23 ± 13
Oxygen	45 ± 13	13 ± 7	59 ± 9	18 ± 6	ND	ND
Anaerobic	ND	19 ± 11	ND	17 ± 5	ND	ND
Air, glucose	ND	ND	36 ± 8	33 ± 10	ND	ND

Table 3.1. Summary of measured dimensions of zones of active DNA replication in *S. epidermidis* colony biofilms and of active protein synthesis and DNA replication in *S. aureus* colony biofilms. The mean and standard deviation are reported. ND, not determined.

Oxygen is Locally Depleted in Biofilms

Local oxygen concentrations within staphylococcal colony biofilms were measured with microe-lectrodes (Figure 3.8). Oxygen penetrated approximately 60 μm into biofilms formed by either *S. epidermidis* (Figure 3.8A) or *S. aureus* (Figure 3.8B). These measurements show that the lower two-thirds of these colony biofilms were anoxic. The dimension of the zone of respiration can be determined from these profiles by computing the local second derivative of the oxygen concentration profile. This quantity represents the curvature of the oxygen concentration data and is proportional to the local reaction rate of oxygen. The width of the zone of respiratory activity was computed at half peak height on the positive curvature of the second derivative of oxygen concentration. The dimension of the zone of respiratory activity measured in this way was 38 ± 2 μm in *S. epidermidis* colony biofilms and was 19 ± 8 μm in *S. aureus* colony biofilms.

The penetration of oxygen into a biofilm is governed by a reaction-diffusion interaction. As oxygen diffuses into the biofilm it is consumed by respiring bacteria. The relative rates of oxygen diffusion and oxygen consumption determine the extent of its penetration. The depth of oxygen penetration is accessible theoretically through the following equation

$$a = \left(\frac{2 D_e S_o}{k_o} \right)^{1/2}$$

where a is the penetration depth of the reacting solute, D_e is the effective diffusion coefficient of the solute in the biofilm, S_o is the solute concentration at the biofilm interface, and ko is the volumetric reaction rate of the solute inside the biofilm. The equation above follows the assumption of zero-order kinetics (rate of reaction is independent of substrate concentration). According to this analysis, the reacting solute will be depleted at some point in the biofilm, provided the biofilm is thick enough (Stewart, 2003).

Independent estimates of each of parameters in this equation were made to enable an a priori calculation of oxygen penetration depth. The diffusion coefficient of oxygen (D_{aq}) in water at 37°C is 2.68 x 10^{-5} cm^2 s^{-1}. The ratio D_e/D_{aq} for oxygen in biofilm averages 0.57. This yields a value of the effective diffusion coefficient (De) in the biofilm of 1.53 x 10-5 cm^2 s^{-1} (Stewart, 2003). The concentration of dissolved oxygen at the biofilm-air interface was taken as 6.0 mg l^{-1}, which is the equilibrium concentration at the barometric pressure in Bozeman, Montana. The rate of oxygen consumption (r_{02}) within a whole colony biofilm was determined to be 0.116 mg h^{-1} by respirometry. This is the rate where oxygen consumption plateaus indicating the onset of mass transfer limitation. This occurred at the colony age between 14 and 19 h. The volume of a colony biofilm (V_b) was measured to be 1.192 x 10^{-3} cm^3. Given these approximations dividing r_{02} by V_b, k_o was estimated, to have a value of the predicted penetration depth of oxygen in a *S. epidermidis* biofilm is 26 μm.

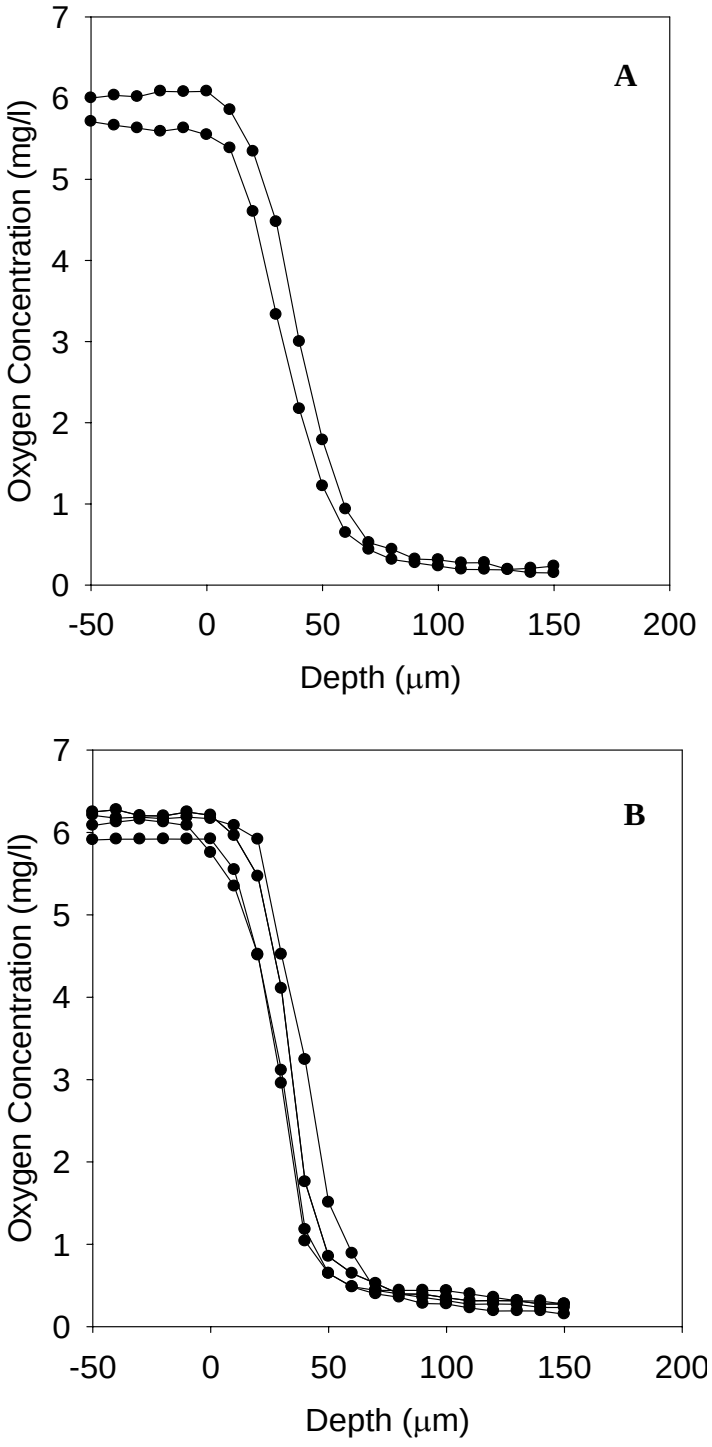

Figure 3.8. Oxygen concentration profiles in *S. epidermidis* (A) and *S. aureus* (B) colony biofilms.

DISCUSSION

Anabolic and respiratory activities in staphylococcal biofilms are highly stratified. Regions of metabolic activity are restricted to the nutrient or oxygen source interface. These regions are a few tens of microns in dimension. In the experiments reported here, zones of anabolic activity were less than about 60 μm wide. These results demonstrate conclusively the presence of metabolically active cells in the biofilm.

These results also imply the existence of a substantial population of inactive cells in the biofilm. In *S. epidermidis* colony biofilms, DNA synthetic activity was detected in a 31 μm zone at the air interface of the colony and a 16 μm zone at the membrane interface (Table 3.1). The average thickness of the biofilm was 153 μm, so one can estimate that an internal region of 106 μm, or 69% of the total biomass thickness, was dominated by inactive cells. Similarly, in *S. aureus* colony biofilms, protein synthetic activity was detected in a 38 μm zone at the air interface of the colony and a 14 μm zone at the membrane interface (Table 3.1). The average thickness of the *S. aureus* biofilm in this case was 173 μm, with an estimated inactive centrally located stratum of 121 μm, or 70% of the total biomass thickness. However, cells that were dispersed before inducing with tetracycline had a percentage of 57% of total cells with GFP expression. This implied that there were at least 27% of total cells that were viable but inactive in intact biofilms.

It is possible that bacterial cells in such inactive regions are still viable. This is suggested by the fact that additions of glucose or pure oxygen to the system expanded the

zone of anabolic activity into regions that were previously inactive, but by no means completely stimulated the entire colony. This shows that at least some of the cells in an inactive region can be stimulated to become active when nutrients or oxygen are made available. It is possible that some of the cells in inactive regions are dead. It can be concluded that staphylococcal biofilms are composed of physiologically heterogeneous populations that include active and also inactive cells.

The double-banded patterns of anabolic activity in colony biofilms can be interpreted in the following way. At the membrane interface of the biofilm, no oxygen is available and the bacteria grow by fermentation. Once fermentable carbon sources have been exhausted no further growth is possible except along the air interface of the biofilm where oxygen is available. At this location, bacteria grow aerobically on non-fermentable carbon sources. In the interior stratum of the biofilm where both oxygen and fermentable carbon sources are absent, bacteria are metabolically inactive. Similar twin bands of fermentative and aerobic activity have been inferred previously in the study of *Klebsiella pneumoniae* colony biofilms (Wentland et al., 1996; Zahller et al., 2002; Anderl et al., 2003). In biofilm systems in which carbon sources and oxygen are delivered to the same interface, a single band of anabolic activity is observed. It is possible, however, that this activity is actually a contiguous layer of aerobic growth, at the biofilm surface, and fermentative growth, just below the aerobic layer, that are seamlessly adjoined (Figure 1.1). The data reported here do not afford a test of this hypothesis because the BrdU labeling and GFP induction techniques do not discriminate between aerobic and anaerobic anabolism.

Measurements of the dimensions of the zones of DNA synthetic activity, protein synthetic activity, and oxygen respiration correspond. For example, in *S. epidermidis* colony biofilms grown in air, the zones of DNA synthetic activity and active respiration along the air interface of the biofilm were between 31 and 38 μm in width. Similarly, *S. aureus* colony biofilms grown in air, the zones of DNA synthetic activity, protein synthetic activity, and active respiration along the air interface of the biofilm were between 19 and 38 μm in width. In *S. aureus* colony biofilms in which the BrdU labeling and GFP induction techniques were applied to the same colony, the patterns of these two anabolic activities were similar (Figure 3.4).

There are relatively few experimental visualizations of general anabolic activity in biofilms. Besides the investigations of *K. pneumoniae* biofilms mentioned above, most studies have focused on *Pseudomonas aeruginosa* biofilms. These investigations have demonstrated oxygen concentration gradients (Xu et al., 1998; Walters et al., 2003; Werner et al., 2004), localized protein synthetic activity as mapped by induction of alkaline phosphatase (Xu et al., 1998) or GFP (Walters et al., 2003; Borriello et al., 2004; Werner et al., 2004), and growth rate as revealed by a growth rate dependent promoter fusion to an unstable GFP (Sternberg et al, 1999). Collectively the research on *P. aeruginosa* biofilms indicate stratified activity located adjacent to the source of oxygen. Hardly any investigations on spatial patterns of growth activity have been performed on staphylococcal systems. In Yarwood et al., (2004), the effects of the accessory gene regulator (*agr*) quorum-sensing system in the development of *S. aureus* biofilms was investigated by employing GFP induction. GFP was expressed in actively growing

regions of the biofilm and upon which suitable conditions within an adequately large cluster of actively growing cells, expression of quorum controlled genes will be activated. However, quantitative measurements of these activities were not reported. In another study, the analysis of DNA synthesis during sporulation in *Bacillus subtilis* by using BrdU labeling was performed (Binnie and Coote, 1983). Nevertheless, spatial activity of DNA replication was not explored.

The patterns of respiratory and anabolic activity observed in staphylococcal biofilms are consistent with a reaction-diffusion interaction governing the access of nutrients and oxygen into the biofilm. For oxygen in particular, sufficient information is available to make the analysis quantitative by solving the differential equation that describes simultaneous Fickian diffusion and oxygen reaction (Stewart et al., 2000; Perez et al., 2005). Oxygen penetration depths calculated in this way (26 μm) are in good agreement with the experimentally measured dimensions of zones of respiratory activity (19 to 38 μm), DNA synthetic activity (25 to 31 μm), and protein synthetic activity (38 μm) measured at the air interface.

Reaction-diffusion theory predicts that oxygen penetration depth should increase in proportion to the square root of the interfacial oxygen concentration. Experiments that substitute pure oxygen for air, representing an oxygen concentration ratio of 100/21, are expected to result in an increase in the depth of oxygen penetration by a factor of $(4.76)^{1/2}$ or 2.2. We found factors of 1.5 and 1.6 for the expansion of zones of DNA synthetic activity and protein synthetic activity, respectively, comparing biofilm growth in oxygen to growth in air. In an analogous experimental comparison of active regions in *P.*

aeruginosa biofilms grown in pure oxygen and ambient air environments, a factor of 1.6 for the ratio of the width of the active zones under these two conditions was reported (Xu et al., 1998). One reason why experimentally determined factors are smaller than the theoretical ratio of 2.2 is that the calculated ratio assumes that the rate of oxygen utilization does not depend on the oxygen concentration. If in fact oxygen consumption rate increases with increased oxygen concentration, this would tend to yield thinner than calculated bands of bacterial activity.

The large number of individuals with suppressed immune systems as an outcome of autoimmune disease, therapy for cancer, or as a result of AIDS has resulted in a population vulnerable to relatively non-virulent microorganisms. These developments, coupled with the emergence of bacterial strains resistant to antibiotics have called for a pressing need to improve methods for the diagnosis, treatment, and control of bacterial infections. The recent advances in modern molecular techniques have certainly eased the process to image bacterial cells in diverse conditions, thus enabling investigators to characterize the growth status of microorganisms in biofilm specimens.

An immediate practical implication of this work is to the understanding of antimicrobial tolerance exhibited by microorganisms in biofilms. An inactive subpopulation harbored within a biofilm is a plausible contributing factor to the recalcitrance of biofilm infections. If inactivity is an important protective mechanism, then surely there are avenues to interdicting this protection. What nutritive and other cues are needed to awaken inactive bacteria and render them susceptible to antimicrobial agents? What specific molecular defenses are deployed when cells enter an inactive state

and how might these defenses be subverted? Which antimicrobial agents are, relatively speaking, effective against inactive cells? Improved approaches for controlling biofilm infections may turn on the answers to such questions, which will facilitate the overall understanding of the inherent physiological heterogeneity that is likely to characterize most biofilms.

CONCLUSIONS

- Anabolic and respiratory activities in staphylococcal biofilms are highly stratified.
- BrdU labeling and GFP expression can be used to map patterns of growth activity. These techniques are generic and may find application in various biofilm reactor systems.
- A substantial fraction of the biofilm cell population exists in an inactive state.
- The double-banded patterns of anabolic activity in colony biofilms are interpreted as indicating a fermentative growth at the nutrient interface and aerobic growth at the air interface of the biofilm.
- Measurements of the dimensions of the zones of DNA synthetic activity, protein synthetic activity, and oxygen respiration correspond.
- Patterns of respiratory and anabolic activity observed are consistent with reaction-diffusion interaction governing the access of nutrients and oxygen into the biofilm.

REFERENCES

Anderl, J. N., Franklin, M. J., and Stewart, P. S. (2000). Role of antibiotic penetration limitation in *Klebsiella pneumoniae* biofilm resistance to ampicillin and ciprofloxacin. J. Antimicrob. Chemother. *44*, 1818-1824.

Anderl, J. N., Zahller, J., Roe, F., and Stewart, P. S. (2003). Role of nutrient limitation and stationary-phase existence *in Klebsiella pneumoniae* biofilm resistance to ampicillin and ciprofloxacin. J. Antimicrob. Chemother. *47*, 1251-1256.

Artusson, V., Finlay R. D., and Jansson, J. K. (2005). Combined bromodeoxyuridine immunocapture and terminal-restriction fragment length polymorphism analysis highlights differences in the active soil bacterial metagenome due to *Glomus mosseae* inoculation or plant species. Environ. Microb. *7*, 1952-1966.

Bateman, B. T., Donegan, N. P., Jarry,T. M., Palma, M., and Cheung ,A. L. (2001). Evaluation of a tetracycline-inducible promoter in *Staphylococcus aureus* in vitro and in vivo and its application in demonstrating the role of sigB in microcolony formation. Infection and Immunity. *69*, 7851-7857.

Beenken, K. E., Dunman, P. M., McAleese, F., Macapagal, D., Murphy, E., Projan, S. J., Blevins, J. S., and Smeltzer, M. S. (2004). Global gene expression in *Staphylococcus aureus* biofilms. J. Bacteriol. *186*, 4665-4684.

Binnie, C. and Coote, J. G. (1983). Density gradient analysis of DNA replicated during *Bacillus subtilis* sporulation. J. Bacteriol. *156*, 466-470.

Borriello, G., Werner, E., Roe, F., Kim, A. M., Ehrlich, G. D., and Stewart, P. S. (2004). Oxygen limitation contributes to antibiotic tolerance of *Pseudomonas aeruginosa* in biofilms. J. Antimicrob. Chemother. *48*, 2659-2664.

Brown, M. R. W., Allison, D.G., and Gilbert, P. (1988). Resistance of bacterial biofilms to antibiotics: a growth-rate related effect? J. Antimicrob. Chemother. *22*, 777-783.

Bryant, R. D., Jansen, W., Boivin, J., Laishley, E. J., and Costerton, J. W. (1991). Effect of hydrogenase and mixed sulfate-reducing bacterial populations on the corrosion of steel. Appl. Environ. Microb. *57*, 2804-2809.

Chopra, I., and Roberts, M. (2001). Tetracycline antibiotics: mode of action, applications, molecular biology, and epidemiology of bacterial resistance. Microb. Molec. Biol. Rev. *65*, 232-260.

Costerton, J. W., Stewart, P. S., and Greenberg, E. P. (1999) Bacterial biofilms: a common cause of persistent infections. Science *284*, 1318-1322.

Devore, J. and Peck, R. (2005). Statistics: the exploration and analysis of data. Crockett, C. and Day, A, ed. (Belmont, CA: Brooks/Cole-Thomson Learning), pp 405-424.

Dolbeare, F., Gratzner, H., Pallavicini, M. G., and Gray, J. W. (1983). Flow cytometric measurement of total DNA content and incorporated bromodeoxyuridine. Proc. Natl. Acad. Sci. USA. *80*, 5573-5577.

Dolbeare, F., and Selden, J.R. (1994). Immunochemical quantitation of bromodeoxyuridine: application to cell-cycle kinetics. In Methods in cell biology. Z. Darzynkiewicz, J.P. Robinson, H.A. Crissman, ed. (San Diego, CA: Academic Press), pp. 297-316.

Donlan, R. M. (2002). Biofilms: Microbial Life on Surfaces. Emerg. Infect. Dis. *8*.

Elias, M. C., Faria, M., Mortara, R. A., Motta M. C., de Souza, W., Thiry, M., and Schenkman, S. (2002). Chromosome localization changes in the *Trypanosoma cruzi* nucleus. Eukaryotic Cell. *1*, 944-953.

Zhang, L., Frank, F., Palmer, L. M., Lonetto, M. A., Petit, C., Voelker, L. L., St. John, A., Bankosky, B., Rosenberg, M., and McDevitt, D. (2000). Regulated gene expression in *Staphylococcus aureus* for identifying conditional lethal phenotypes and antibiotic mode of action. Gene, *255*, 297-305.

Gerdes, H-H., and Kaether, C. (1996). Green fluorescent protein: applications in cell biology. FEBS Letters. *389*, 44-47.

Herman, B. (2001). Fluorescence microscopy. (New York, New York: Bios Scientific Publishers), pp 90-94.

Hodgson, A. E., Nelson, S. M., Brown, M. R. W., and Gilbert, P. (1995). A simple in vitro model for growth control of bacterial biofilms. J. Appl. Bacteriol. *79*, 87-93.

Huang, C. T., Xu, K. D., McFeters, G. A., and Stewart, P. S. (1998). Spatial patterns of alkaline phosphatase expression within bacterial colonies and biofilms in response to phosphate starvation. Appl. Environ. Microbiol. *64*, 1526-1531.

Kuhn, R. H., S. W. Peretti, and Ollis, D. F. (1991). Microfluorimetric analysis of spatial and temporal patterns of immobilized cell growth. Biotechnol. Bioeng. *38*, 340-352.

Inoué, S. (1995). Foundations of confocal scanned imaging in light microscopy. In Handbook of biological confocal microscopy. Pawley, J. B., ed. (New York, New York: Plenum Press), pp 1-14.

Leif, R. C., Stein, J., H., and Zucker R. M. (2004). A short history of the initial application of anti-5-BrdU to the detection and measurement of S phase. Wiley-Liss, Inc. *58A*, 45-52.

Lichtenwalner, R. J., Forbes, M. E., Sonntag, W. E., Riddle, D. R. (2006). Adult-onset deficiency in growth hormone and insulin-like growth factor-I decreases survival of dentate granule neurons: Insights into the regulation of adult hippocampal neurogenesis. J. Neuroscience Research. *83*, 199-210.

Mah, T-F., and O'Toole, G. A. (2001). Mechanisms of biofilm resistance to antimicrobial agents. Trends in Microbiology. *9*, 34-39.

Martiny, A. C., Albrechtsen, H-J., Arvin, E., and Molin, S. (2005). Identification of bacteria in biofilm and bulk water samples from a nonchlorinated model drinking water distribution system: detection of a large nitrite-oxidizing population associated with Nitrospira spp. Appl.Environ. Microb. *71*, 8611-8617.

Nishimura, S., Tsurumoto, T., Yonekura, A., Adachi, K., and Shindo, H. (2006). Antimicrobial susceptibility of *Staphylococcus aureus* and *Staphylococcus epidermidis* biofilms isolated from infected total hip arthroplasty cases. J. Orthopaedic Science. *11*, 46–50.

O'Gara, J. and Humphreys, H. (2001). *Staphylococcus epidermidis* biofilms: Importance and implications. J. Med. Microbiol. *50*, 582-587.

Oike, H., Matsumoto, I., and Abe, K. (2006). Group IIA phospholipase A2 is coexpressed with SNAP-25 in mature taste receptor cells of rat circumvallate papillae. J. Comp. Neuro. *494*, 876-886.

O'Toole, G., Kaplan, H., B., Kolter, R. (2000). Biofilm formation as microbial development. Ann. Rev. Microb. *54*, 49-79.

Paddock, S. W. (1999). An introduction to confocal imaging. Confocal microscopy methods and protocols. In Methods in molecular biology. Paddock, S. W., ed (Totowa, New Jersey: Humana Press), pp 1-34.

Perez, J., Picioreanu, C., and van Loosdrecht, M. (2005). Modeling biofilm and floc diffusion processes based on analytical solution of reaction-diffusion equations. Wat. Res. *39*, 1311-1323.

Pernthaler, A., Pernthaler, J., Schattenhofer, M., and Amann, R. (2002). Identification of DNA-synthesizing bacterial cells in coastal north sea plankton. Appl. Environ. Microbiol. *68*, 5728-5736.

Pernthaler, A. and Pernthaler, J. (2005). Diurnal variation of cell proliferation in three bacterial taxa from coastal north sea waters. Appl. Environ. Microbiol. *71*, 4638-4644.

Poulsen, L. K., G. Ballard, and Stahl D. A. (1993). Use of rRNA fluorescence in situ hybridization for measuring the activity of single cells in young and established biofilms. Appl. Environ. Microbiol. *59*, 1354-1360.

Rani, S. A., B. Pitts, and P. S. Stewart. (2005). Rapid diffusion of fluorescent tracers into *Staphylococcus epidermidis* biofilms visualized by time lapse microscopy. J. Antimicrob. Chemother. *49*, 728-732.

Rice, S. A., Koh, K. S., Queck, S. Y., Labbate, M., Lam., K. W., and Kjelleberg, S. (2005). Biofilm Formation and Sloughing in *Serratia marcescens* Are Controlled by Quorum Sensing and Nutrient Cues. J. Bacteriol. *187*, pp 3477-3485.

Sheppard, C. J. R, and Shotton, D. M. (1997). Confocal laser scanning microscopy. Microscopy Handbooks 38. (New York, New York: Bios Scientific Publishers).

Sternberg, C., Christensen, B. B., Johansen, T., Nielsen, A. T., Andersen, J. B., Givskov, M., and Molin, S. (1999). Distribution of bacterial growth activity in flow-chamber biofilms. Appl. Environ. Microbiol. *65*, 4108-4117.

Stewart, P. S., and Roberston C. R. (1988). Product inhibition of immobilized *Escherichia coli* arising from mass transfer limitation. Appl. Environ. Microbiol. *54*, 2464-2471.

Stewart, P. S., S. F. Karel, and Robertson C. R. (1991). Characterization of immobilized cell growth rates using autoradiography. Biotechnol. Bioeng. *37*, 824-833.

Stewart, P. S., A. K. Camper, S. D. Handran, C.-T. Huang, and Warnecke, M. (1997). Spatial distribution and coexistence of *Klebsiella pneumoniae* and *Pseudomonas aeruginosa* in biofilms. *33*, 2-10.

Stewart, P. S., McFeters, G. A., and Huang, C.-T. (2000). Biofilm control by antimicrobial agents. In Biofilms, J. D. Bryers, ed. (New York, NY: John Wiley & Sons).

Stewart, P. S., and Costerton, J. W. (2001) Antibiotic resistance of bacteria in biofilms. Lancet *358*, 135-138.

Stewart, P. S. (2003). Diffusion in biofilms. J. Bacteriol. *185*, 1485-1491.

Timke, M., Wang-Lieu, N. Q., Altendorf, K. and Lipski, A. (2005). Fatty acid analysis and spoilage potential of biofilms from two breweries. J. Appl. Microb. *99*, 1108-1122.

Toledo-Arana, A., Merino, N., Vergara-Irigaray, M., Débarbouillé, M., Penadés, J. R., and Lasa, I. (2005). *Staphylococcus aureus* Develops an Alternative, *ica*-Independent Biofilm in the Absence of the *arlRS* Two-Component System. J. Bacteriol. *187*, pp 5318-5329.

Walters, M. C., Roe, F., Bugnicourt, A., Franklin, M. J., and Stewart, P. S. (2003). Contributions of antibiotic penetration, oxygen limitation, and low metabolic activity to tolerance of *Pseudomonas aeruginosa* biofilms to ciprofloxacin and tobramycin. J. Antimicrob. Chemother. *47*, 317-323.

Wentland, E. J., Stewart, P. S., Huang, C. T., and McFeters, G .A. (1996). Spatial variations in growth rate within *Klebsiella pneumoniae* colonies and biofilm. Biotechnol. Prog. *12*, 316-321.

Werner, E., Roe, F., Bugnicourt, A., Franklin, M. J., Heydorn, A., Molin, S., Pitts, B., and Stewart, P. S. (2004). Stratified growth in *Pseudomonas aeruginosa* biofilms. Appl. Environ. Microbiol. *70*, 6188-6196.

Wilson, T. (2002). Confocal microscopy: basic principles and architectures. In Confocal and two photon microscopy. Diaspro, A, ed. (New York, New York: Wiley Liss), pp 19-38.

Xu, K. D., Stewart, P. S., Xia, F., Huang, C. T., and McFeters, G. A. (1998). Spatial physiological heterogeneity in *Pseudomonas aeruginosa* biofilm is determined by oxygen availability. Appl. Environ. Microbiol. *64*, 4035-4039.

Xu, K. D., McFeters, G. A., and P. S. Stewart. (2000). Biofilm resistance to antimicrobial agents. Microbiol. *146*, 547-549.

Yao, Y., Sturdevant, D. E., and Otto, M. (2005). Genomewide analysis of gene expression in *Staphylococcus epidermidis* biofilms: insights into the pathophysiology of *S. epidermidis* biofilms and the role of phenol-soluble modulins in formation of biofilms. J. Infect. Dis. *191*, 289-298.

Yarwood, J. M., Bartels, D. J., Volper, E. M., and Greenberg, E. P. (2004). Quorum sensing in *Staphylococcus aureus* biofilms. J. Bacteriol. *186*, 1838-1850.

Zahller, J., and Stewart, P. S. (2002). Transmission electron microscopic study of antibiotic action on *Klebsiella pneumoniae* biofilm. J. Antimicrob. Chemother. *46*, 2679-2683.

Zheng, Z. and Stewart, P. S. (2002). Penetration of rifampin through *Staphylococcus epidermidis* biofilms. J. Antimicrob. Chemother. *46*, 900-903.

Zhu, X. Y., Lubeck, J., and Kilbane II, J. J. (2003). Characterization of microbial communities in gas industry pipelines. Appl. Environ. Microb. *69*, 5354-5363.

Zimmerli, W., Trampuz, A., and Ochsner, P. E. (2006). Prosthetic-joint infections. N. Eng. J. Med. *351*, 1645-1654.